2014

Fabrication of Micropatterns for the Spatial Control of Cell Propagation and DIfferentiation

Mahmoud Moustafa
Virginia Commonwealth University

Fabrication of Micropatterns for the Spatial Control of Cell Propagation and Differentiation

A dissertation submitted in partial fulfillment of the requirements for the degree of Master of Science at Virginia Commonwealth University

by

Mahmoud Moustafa, B.S (Chemical Engineering)

American University of Sharjah, United Arab Emirates, 2011

Director: Dr. Vamsi K. Yadavalli

Associate Professor

Department of Chemical and Life Science Engineering

Virginia Commonwealth University

Richmond, Virginia

August, 2014

Acknowledgements

I would like to thank my advisor Dr.Vamsi Yadavalli for the learning experience, guidance and engagement along the way. I would also like to express my appreciation to the committee members Dr. Raj Rao and Dr. Christopher Lemmon for their presence and insight during my defense. I would also like to thank them for their advice numerous time and allowing me access to their facilities. Financial support and funding for this project was granted by the National Science Foundation.

I am highly grateful to my colleagues and friends who have provided a lot of support and encouragement along this project and to whom I owe a lot of the success related to this work. Thank you to Dr. Nicholas Kurland, Eric McCullough, Woomin Lee, Ahmed Ahmed Elmak, Snehi Shrestha, Venkat Gadepalli, Congzhou Wang and Ramendra Pal.

A special thanks to my parents Esam Moustafa and Fatma Kotb for their unlimited reassurance and comfort. Your prayers are what guided me to the end and I could not ask for a more caring, loving and more supporting family.

Table of Contents

List of Tables

List of Figures

Abstract

FABRICATION OF MICROPATTERNS FOR THE SPATIAL CONTROL OF CELL PROPAGATION AND DIFFERENTIATION

By Mahmoud Moustafa.

A thesis submitted in partial fulfillment of the requirements for the degree Master of Science in Chemical and Life Science Engineering at Virginia Commonwealth University

Virginia Commonwealth University, 2014

Major Director: Dr. Vamsi K. Yadavalli, Associate Professor of Chemical and Life Science Engineering

Abstract Text:

Challenges in the development of successful cell therapies involve engineering and control of cues to regulate the balance between differentiation and self-renewal. However, the complexity of architecture and function make this an intriguing problem in the context of forming functional connections. Here we present the design and fabrication of microstructured scaffolds that present a biomimetic framework along which neural cell lines can organize into oriented constructs. Specifically, we show microfabricated non-linear architectures that promote cellular fate related to propagation of human neuroblastoma cells and directed differentiation towards neurons. By mimicking biological networks that allow for spreading of the cells instead of confining them in a groove or a well, a nonlinear configuration can promote a relaxed, self-supportive cell niche. The tailoring of non-homogeneous adhesion sites via the geometry and the compliance and roughness of the substrate allows a versatile microenvironment that promotes propagation and neuronal differentiation.

Chapter 1: Micropatterning of Cells

1.1. Introduction

Cells growing *in vivo* interact with neighboring cells, the extracellular matrix (ECM) and the accommodating surfaces. These as a whole shape cell fate in terms of division, proliferation and differentiation. *In vitro* cell culture in open space and traditional biochemical studies have traditionally oversimplified such contacts and offer a limited view to the way cells sense and respond to their environment [1]. This has resulted in a generally inaccurate representation of cell surroundings [2]. Micropatterning techniques have been suggested as a means to better mimic cell growth conditions by providing spatial cues at the micro and nanoscales similar to those encountered *in vivo* [1, 3]. Integrating microfabrication strategies from the semiconductor industries with cell culture, makes it possible to form various efficiently controlled cell cultures down to dimensions that are physiologically relatable to individual cells [3]. Such incorporation may involve geometrically defined adhesive regions that encourage specific attachment through surface chemistry or physical barriers [4]. This results in better regulation of cell response and fate through the biochemical structure and topology of the *in vitro* environment [4, 5]. For instance, patterned cells growing in microchannels enjoy a significantly higher surface area to volume ratio than cells cultured openly on tissue culture. This is useful in cases where the substrate is gas-permeable owing to effective mass transport of gases [2].Furthermore, the ability of most animal cells to grow on two-dimensional surfaces has paved the way for patterning in particular and its applications towards three-dimensional cultures [3].

1.2. Applications of cell micropatterning

1.2.1. Fundamental studies in cell biology

Cell micropatterning is vital for studies in cell biology as a tool to control the size and spatial orientation of cells [6]. Beyond direct applications in tissue engineering, artificial organs and microarray technologies, precisely controlling the position of cells also has great potential in furthering our understanding of fundamental intercellular interactions and cues [7-11]. Studies on cell contact and adhesion continue to develop with the aid of micropatterning. Cell adhesion is a function of the relationships between the extracellular matrix and cell membrane protein integrin responsible for focal adhesions. This phenomenon, together with cell contact and spreading, play a crucial role in signal transduction, metabolism and therefore how the cell behaves. A clearer and more specific view of how the focal adhesion complex (FAC) works regarding its assembly and reaction to various substrates has been provided [1, 12]. Cell migration can also be examined in response to shape changes induced through micropatterning. It has also been found that cell spreading is what regulates whether the cells proliferates or undergoes apoptosis (programmed cell death) through the available area and change in cell alignment to match the space [1, 13].

1.2.2. Tissue engineering

Specific placement of cells to form spatially organized patterns is required for tissue engineering applications [14, 15]. The aim is to ultimately be able to implant systems in bodies and help construct tissues *in vitro* more efficiently to mimic the *in vivo* functions and structure [16, 17]. This would mean the ability to replace or repair unhealthy tissues and treat degenerative diseases

such as Alzheimer's and heart disease. In order to grow tissues that are physiologically viable and capable of preserving functionality, cell relations with other types of cells and the governing material are vital in a practical tissue model. Patterning techniques consequently can help understand such relationships through organized control of different cell types on a single substrate which plane co-culture systems fail to provide [1, 6, 13, 15].

Topography has already been proven to influence differentiation of stem cells and even improve yield in certain directions depending on the intent. For instance, aligned fibrous matrices and gratings exhibited higher neural differentiation rate from human embryonic stem cells (hESCs) than un-patterned substrates [18, 19]. Incorporating micropatterning through artificial ECMs with adult or embryonic stem cells can therefore control their interactions and fate for regenerative medicine purposes [20]. In another study, microengineered cardiomyocytes on biocompatible substrates have shown promise in efforts to maintain myocardial properties *in vitro* and provide a means for repairing damaged hearts through implantation [21]. A lot of progress has been made in 2D microfabrication for tissue engineering purposes but future directions will aim to provide a 3D cellular environment which represents more of the physical and chemical cues [22].

1.2.3. Cell-based biosensing

Biosensors based on cells revolve around stimulating them individually and recording the feedback which indicates the need for precise arrangement of the cells to facilitate access [14, 15]. Using cell-based biosensors offers higher sensitivity, more stable environment and wider

range of detection compared to molecular ones, while yielding results faster than whole animal studies [23-25]. Pharmaceutical drug screening and toxin detection are a major application where immobilized cells can be exposed to analytes and monitored for changes in viability or metabolism. Neurons, for example, would respond to chemical variations in the environment through electrical signals which can be quantified and reported [1, 6] Various micropatterning techniques have therefore been attempted and incorporated with electrochemical technologies to improve cell-based biosensors' performance [23].

1.3. Currently used techniques to spatially pattern cells at the micro and nanoscales

1.3.1. Soft lithography

Soft lithography collectively describes a group of micropatterning approaches that rely on the use of an elastomeric or soft material as replica mold at some point [1, 11] . Photolithography is only included in making the masters which embody features limited by the photomask resolution. Poly (dimethylsiloxane) (PDMS) is also the most commonly used elastomer due to its flexibility, cost effectiveness and endurance for repeatable use without major degradation over numerous months. Microcontact printing, microfluidic patterning and stencil patterning are the main branches of soft lithography used for cellular and protein micropatterning [6, 15, 26] .

1.3.2. Microcontact printing (μCP)

Microcontact printing is regarded the most commonly used soft lithography technique and its desirability stems from being simple and cost effective. It is also compatible with various

substrates and flexible when it comes to the choice of material to be imprinted [11, 26]. μCP involves forming an elastomeric stamp first by casting a liquid polymer, usually poly (dimethylsiloxane) [6, 11], on the microstructured master prepared using photolithography. Once cured, a replica is obtained which is then "inked" with molecular layer to be transferred such as an alkanethiol in ethanol to support cell attachment to the –CH3 terminated thiols [1, 15].This is followed by the actual stamping step to print the pattern on the substrate by contact and letting it dry. Finally, if the substrate does not resist cell adhesion by nature, it can be immersed in a second type of solution that would backfill the space such as PEG terminated thiols. The result would therefore be a surface with cytophilic patterns surrounded by cytophobic space required to organize the cells accordingly [1, 6, 13, 15, 26]. Microcontact printing offers the highest resolution in soft lithography is particularly convenient when up to two types of molecules need to patterned [6, 15].

1.3.3. Microfluidic patterning

Microfluidic patterning is similar to μCP in the sense that it uses replica molds which are brought in contact with the substrate. However, this technique restricts fluid flow through microchannels to transfer the biomolecules onto the surface rather than stamping [1, 13, 15] . The solution can be introduced by capillary action or a pump for pressure driven flow when the fluid is viscous or larger areas are needed [6, 26] This forms patterns of the dissolved molecules on the substrate where it does not contact the mold that would promote selective cell attachment [11]. The microfluidic technique, like μCP, is considered inexpensive and relatively easy to implement. It is also the most suitable soft lithography approach for patterning several types of molecules in

parallel and therefore performing subcellular studies [26]. Furthermore, a drying step is not required and it is therefore more compatible with delicate biomolecules like proteins and enzymes which can maintain their functionality [1, 15].

1.3.4. Stencil patterning

This method relies on physical barriers rather than surface chemistry and is accomplished fabricating stencils with through holes in a similar manner to stamps. PDMS is again frequently used for this purpose since it also locks by nature to most dry surfaces and is not optimal for cell adhesion due to its hydrophobicity. Typically, PDMS prepolymer is poured on the master without covering the micropatterns and peeled off once cured to form a stencil. Cells therefore attach where the holes are and on the substrate below. Once the stencil is removed it leaves a pattern of cells with the same shapes [1, 6]

1.3.5. Photolithography/Photochemistry

Photolithography was traditionally developed for use in the semiconductor industry and for fabricating microcircuits, with silicon being the commonly used substrate. It is a technique that is now very widely implemented for protein and cell patterning mainly due to the high accuracy and resolution it offers and not just limited to masters for soft lithography [10, 27-29]. The concept revolves around the substrate being spin coated with a light sensitive polymer or photoresist to form a uniform thin layer. The coated surface is then brought close or in contact with a photomask and exposed to ultraviolet light. Depending on the photoresist used, the light

will selectively either polymerize (negative resist), or degrade it (positive resist), transferring the pattern from the photomask onto the substrate [1, 26, 29]. Like microcontact printing and microfluidic patterning, the result is a cell adhesive region surrounded by a cell resistant one. In addition, photolithography is compatible with multiple substrates from glass to polymers and offers the capability to pattern larger areas than soft lithography with more complex features [13]. Initially, the cost of having to operate in clean rooms and have access to expensive facilities was a setback in the applicability of this method [15]. However, several variations such as projection and transparency-based photolithography have since been developed, which remove the need for a clean room and make it less expensive and time consuming [11, 29-31].

1.4. Objectives of this project

The development of methods to spatially control cell growth in two and three dimensions has been a fundamental challenge for *in vitro* research and simulating *in vivo* cellular microenvironments [2, 32]. Maintaining precise uniformity over large areas, which is characteristic of live tissue, is still a challenge and is vital for application. According to existing results, as the development of fabrication techniques in micro scale and methods in cell biology continues, cell micropatterning techniques will allow us to have improved control of cell behaviors [1]. Cell micropatterning is still grossly oversimplified compared with the in vivo scenario and despite the abundance of techniques available; each has certain disadvantages that hinder progress. Microcontact printing is too influenced by the characteristics of the stamp material and the tradeoff between a softer, elastic stamp which would be highly adaptable to the substrate in contact and a rough stamp that would allow more accurate patterning [26].

Furthermore, repeatability over large areas is hard to achieve and having more than two inks for co-culture systems can be complicated due to concerns over diffusion and the need for a succession of stamping stages [11, 13, 15]. Microfluidic patterning's use of fluid flow might allow several types of molecules to be patterned but it is also limited to open structure composed of channels and offers less versatility [1, 6, 11, 15, 26]. In addition, photolithography is not well suited for patterning on constructs that have previously been functionalized with delicate ligands [11] . However, majority of the holes in stencils are simple shapes like circles and squares. If the shapes have many corners, they can be easily damaged while peeling PDMS off the mold. [1, 6] This means ongoing advancement in the existing techniques to counteract their disadvantages and striving to develop new ones.

Here a combination of different techniques outlined above is used to develop a facile strategy for the micropatterning of cells via physico-chemical barriers. Specifically, PDMS is used as a versatile underlying substrate for cells while the barriers are formed using protein-resistant poly (ethylene glycol) diacrylate (PEGDA) patterns. This is shown over large areas to be more feasible as a technique for tissue engineering. To better recapitulate complex spatial designs, the use of "open-architectures" for cell growth is investigated, which marks a different direction from the traditional geometric patterning presented in several studies. These results are demonstrated on different cell lines with neuronal cells being the focus to develop systems for neural regeneration. These studies will result in creating engineered substrates that can be modulated in terms of mechanical properties, micro and nano structure as well as spatial architecture to form systems for the control of spatial growth in two and (eventually) three dimensions.

Chapter 2: Strategies for patterning of structural features at the microscale

2.1. Introduction

Poly (dimethylsiloxane) (PDMS) is a polymer that has been conventionally used for microfluidic and bioengineering purposes. PDMS has unique properties including its optical transparency, biocompatibility, flexibility, oxygen permeability, durability and low cost which have led to its widespread use in cell culture [9, 30, 33]. Such characteristics provide advantages in comparison to microfabrication attempts on more rigid substrates such as polystyrene, silicon, glass and gold [6, 16]. PDMS consists of a precursor containing dimethylsiloxane oligomers with vinyl-terminated end groups mixed with a curing agent that contains a crosslinking agent and an inhibitor. Upon crosslinking, the oligomers undergo hydrosilylation and form a Si-C bond [34, 35]. Recent literature has mostly demonstrated micropatterning without using adhesive inhibitors [8, 36]. PDMS stamps provide physical localization only which can be insufficient. These stamps which utilize extracellular matrix components such as laminin for cell attachment without further surface modification are limited to about 50 μm features [37]. In general, this has been a challenge in the application of PDMS to micropatterned cell culture as patterns are only able to be formed over a few millimeters (mm). In contrast for more general applications, it is desired to provide micro and nanostructural control often over several centimeters (cm). Photolithography as an indirect patterning method, where the substrate is prepared followed by cell attachment, has a major advantage of the ability to obtain high resolution patterns over large areas [11, 15] Other

micropatterning techniques currently used include soft lithography [38], stencils [9] , microfluidic devices [39, 40] and colloidal lithography [41].

To create barriers for cell growth, while encouraging proliferation on the PDMS matrix it is necessary to create barriers. Immobilizing polyethylene glycol (PEG) polymers to form hydrophilic, neutral charged hydrogels has been widely used as a method to repel non-specific protein adsorption and cell attachment [7, 26, 42-45]. For instance, successful micropatterning of murine 3T3 fibroblasts on glass was shown, with PEG offering great resistance to cell adhesion and enabling specific, flexible patterning [7]. High density PEG layers were also shown to decrease nonspecific adsorption of DNA by 14-fold [43, 46]. Polyethylene glycol diacrylate (PEGDA) specially has been proven to be very effective with long-lasting hydrophilic properties [30]. Alternatives such as polyethylene glycol methacrylate (PEGMA) on the other hand, suffered from gradual loss of hydrophilicity. Cell patterning using oxygen plasma can cause oxidation of biologically modified regions during reactive plasma treatment. Further, the PEG film generated by patterned etching using oxygen plasma limited the smallest feature to 15 μm due to distortion of the elastomeric masks [47]. Creating monolayers using PEGMA, may yield fragile patterning and cannot withstand physiological or microfluidic shear stresses [48]. Other options that involve dynamic surface modification such as plasma oxidation of PDMS to increase hydrophilicity followed by perfluorosilane functionalization are only temporary [43, 49] and not suitable for patterning applications.

Further, photografted microstructures on PDMS are for the most part restricted to simple geometric patterns such as circles and squares. Here, a PEGDA hydrogel photografted on PDMS

with a 1 centimeter grid of 25 and 50 micrometer micropatterned lines. Owing to the versatility of photolithography, it is possible to form shapes of any complexity. As show below, we take advantage of this to form open network architectures for better cell proliferation. Culturing the fibroblasts on these fibronectin coated patterns shows homogenous cell adhesion and growth over a macro scale bringing microfabrication a step closer to mass production over much larger scales for medical use.

2.2. Materials and methods

PDMS prepolymer and curing agent (Sylgard 184) were obtained from Dow Corning (Midland, MI, USA). PEGDA (number average molecular weight, 575, 3-(tricholorsilyl) propyl methacrylate (TPM) and albumin-fluorescein isothiocyanate conjugate were purchased from Aldrich (St. Louis, MO, USA). Benzophenone and acetone were obtained from Alfa Aesar (Ward Hill, MA, USA). Benzyl alcohol, Sodium periodate ($NaIO_4$), methanol, paraformaldehyde powder and Phosphate buffered saline (PBS) solution (10X) were obtained from Fisher Scientific (Fair Lawn, NJ, USA) and used as received.

A bright field high reflective chromium photomask was designed using CleWin to include a 2.25 cm^2 grid consisting of 50 and 25 μm lines separated by 150 μm squares. The fabrication process was then conducted using a Heidelberg μPG 101 micro pattern generator under 5 mW exposure at 25% intensity and with 1X energy factor operating in unidirectional mode. In order to process the photomask, it was developed for 1 minute in the micro-chrome developer PPD-450 (HTA Enterprises, San Jose, CA, USA) while monitoring the mask for the development of the fine

features. Etching was performed for 4 minutes the chrome etchant CEP-200 (Microchrome Technology Inc., NY, USA) and finally the mask was placed in the positive resist stripper PRS-100 (HTA Enterprises, San Jose, CA, USA) for 8 minutes. A stop bath of deionized water was included between each step for rinsing and the mask was inspected following the development and etching stages under the microscope with low light exposure to ensure the fidelity of the features.

Microscopic glass slides were diced into 0.8 inch^2 samples and rinsed thoroughly with deionized water and ethanol. Substrates were then dried at 150 °C on a thermal plate and immersed in "piranha" solution for 30 minutes. The solution is composed of 98% sulfuric acid and hydrogen peroxide (Fisher Scientific, NJ, USA) at a 3:1 ratio. This is meant to introduce hydroxyl groups necessary for silane treatment. The slides were rinsed again thoroughly and dried. This was followed by 12 hours of TPM chemical vapor deposition to form Si-O-Si bonds on the hydroxylated substrate and therefore a TPM monolayer that would allow PEG-DA to establish covalent bonds with the methacrylate groups [45]. Slides were then rinsed with deionized water and hexane then air dried while covered with aluminum foil.1 ml of 40wt% PEGDA solution was prepared by dissolving 400 µl of PEGDA, 10 µl of the photoinitiator Darcocur (Ciba Specialty Chemicals) in water, while the 60% PEGDA solution had 600 µl of PEGDA. The solution was photopolymerized through a photomask using a 365 nm, 500 mW/cm^2 light source (OmniCure S1000 100 W lamp). 20 µl of the solution was spread on the glass surface and exposed using contact lithography at 5% intensity for 3 seconds while maintaining a 2.5 inches distance between the light source and sample.

To prepare the 10:1 (mass ratio of base to curing agent, respectively), 20:1 and 5:1 PDMS samples, 12.5 g of pre-polymer was mixed with 1.25 g, 0.625 g and 2.5 g of curing agent respectively and added to a 100 mm plastic petri dish. After overnight curing at 62°C, the PDMS was peeled off and diced into square samples. The 10:1, 20:1 and 5:1 PDMS slabs were then immersed in a 10 wt% benzophenone solution in acetone for 2 minutes and 1 minute respectively. The samples were rinsed with methanol and air dried. The 5:1 PDMS samples were also rinsed in 50 wt% acetone solution and stored in water overnight. 1 ml of 40wt% PEGDA solution was prepared by dissolving 400 µl of PEGDA, 10 µl of 100mM $NaIO_4$ (1 mM) and 50 µl of benzyl alcohol (5wt%) in water and 65 µl of the reaction solution was spread on the PDMS surfaces. The exposure conditions were optimized to obtain large patterned areas over several mm. For instance, the 10:1 samples were exposed at 75% of max output for 8.5 seconds, 6 times. The first three runs had 1 minute intervals while the last three were back to back. The 20:1 and 5:1 samples on the other hand were exposed at 100% of max intensity for 9 seconds with 7x repeats. A schematic in **Figure 2.1** shows the steps involved in obtaining a stable, micropatterned PEGDA hydrogel on PDMS. Glass slides and PDMS samples were each covered with 1 mg/ml of albumin-fluorescein isothiocyanate (FITC-BSA) conjugate for 30 minutes before being examined under a fluorescence microscope (Nikon ECPLISE TE2000-U).

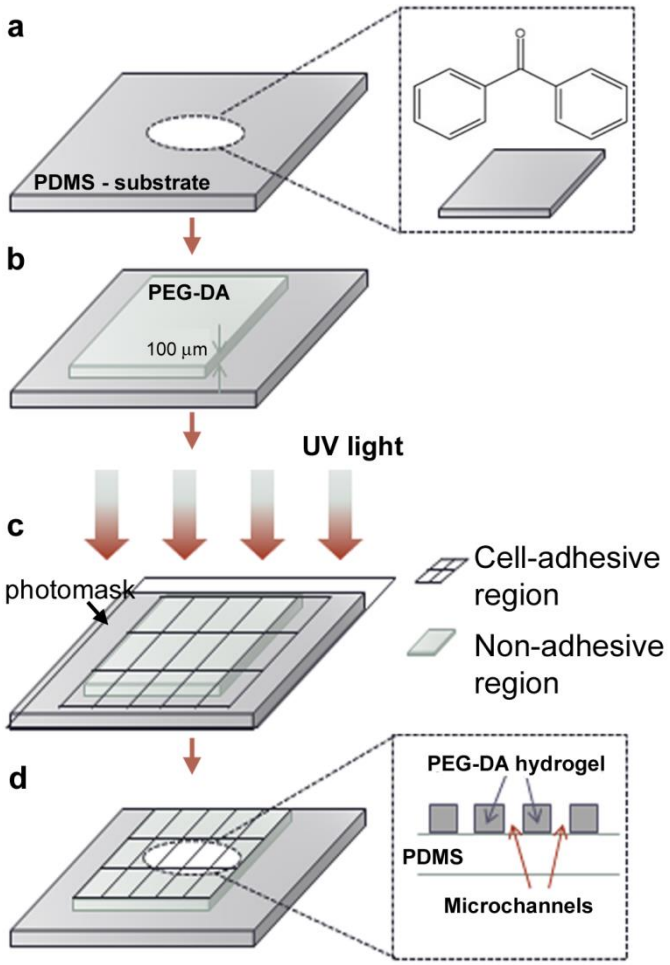

Figure 2.1. (a) Benzophenone diffusion on to PDMS surface. (b) PEGDA with uniform layer of 100 µm thickness. (c) Exposure of UV through bright field mask. (d) Hydrophilic hydrogel constructed on the substrate for micropatterning of cells.

The mechanical properties of crosslinked films of PDMS were measured using AFM-based nanoindentation (MFP-3D, Asylum Research, Santa Barbara, CA). All samples were indented using an AC160 TS cantilever (Olympus Research, Tokyo, Japan) with nominal spring constants varying from 30-40 N/m. The actual spring constants were determined using the thermal fluctuation method [50]. 6 times of measurements on hard mica surface were conducted to obtain the average calculated spring constant as the value used for analysis prior to every nanoindentation experiment. For the nanoindentation experiment, each PDMS sample was

indented in air with ~30 indents at ~30 different spots on the surface by constant force mode (150 nN). The Young's modulus and stiffness were obtained by fitting Oliver-Pharr model on each curve [51] in Igor Pro 6.22 A (Wavemetrics Inc, OR).

2.3. Results and discussion

In order to form high resolution architectures that have high resolution, fidelity and stability over large areas and long periods of time, it was necessary to optimize every step of the photografting process. Previous studies reported their experiments were conducted in UV chamber for duration up to 10 minutes [30]. Operating at an intensity of 50 mW/cm^2, exposing the sample for more than 2 minutes (and up to 10 minutes) resulted in stable, hydrophilic PEGDA hydrogels for months. We found that extending exposure time led to thermal polymerization and the hydrogel turned cloudy even at such a low intensity. Importantly, the cloudy hydrogel began delaminating once it was placed in water or 1X PBS at 37 °C in just a couple of days. This is probably due to the heat generated during the photopolymerization steps. The UV polymerization without thermal polymerization was therefore required for successful, covalently bonded hydrogel to the substrate in order to study protein and cell adhesion. The distance from the lamp, intensity of the light source and time of exposure all contribute to the amount of light energy transferred to the substrate. The intervals between exposures allowed the heat energy to dissipate between UV polymerization. In addition, the amount of benzyl alcohol, which acts as a chain transfer agent and aids in the diffusion of the reactive monomers to PDMS surface by decreasing the solution viscosity, added in the monomer solution for this study was considerably more than the standard concentration of 0.5 wt% [30, 31, 52]. This contributed to ensuring stable attachment of the

hydrogel to PDMS which delaminated otherwise given the large area. To ensure the stability of the hydrogel and viability of the sample for cell culture, once again, it was kept in a 37 °C water bath for 7 days. The hydrogel remained intact and the channels maintained their width.

Manipulating the precursor to cross-linker ratio results in varying PDMS stiffness and dictates the quantity of uncrosslinked oligomers [32, 53]. Previous reports indicated that increasing the base:crosslinker ratio by 5-fold resulted in the elastic modulus decreasing by 40-fold [54], while an increase in the amount of crosslinker resulted in stiffer substrates [55, 56]. Optimal PDMS, in terms of cross-linking density and amount of uncrosslinked oligomers, is standardized as 10:1 (base:crosslinker). Excess curing agent, as in the 5:1 PDMS, means a stiffer substrate under extended processing time since further crosslinking is promoted. Surplus in the precursor, as in the 20:1 PDMS, leads to a softer substrate due to insufficient amount of curing agent and presence of unlinked vinyl terminated oligomers [34]. Both cases are characterized with uncrosslinked, low molecular weight oligomers that influence the surface chemistry and therefore cell behavior on the substrate. While temperature and curing time also contribute to the rigidity of PDMS, they were kept constant at 62 °C for 24 hours (overnight). The lower the temperature, the higher the curing time needed and this ensured further crosslinking for either component in excess while maintaining the stiffness differences. **Table 2.1** demonstrates these variances through the Young's modulus obtained using AFM-based nanoindentation, which increased with reduction in the precursor to crosslinker ratio.

Table 2.1: Elastic moduli and stiffness of PDMS with varying base to curing agent ratios

Base:CA	*Modulus (MPa)*	*Stiffness (N/m)*
5:1	*6.10 ± 0.11*	*1.90 ± 0.04*
10:1	*2.95 ± 0.05*	*1.35 ± 0.02*
20:1	*1.38 ± 0.05*	*1.10 ± 0.04*

Earlier studies showed success in micropatterning PDMS down to a few microns in mostly systems which did not involve non-adhesive barriers and were limited to confined areas [30, 31, 33, 37]. However, the stability of the resolution under several environmental or mechanical cues remains questionable and is regarded a limitation for long cellular and high-throughput studies. **Figure 2.2(a)** shows large scale patterning (> 1 mm^2) on PDMS, reaching a micropatterned area of 2.25 cm^2 with the 25 and 50 μm channels maintaining their fidelity uniformly throughout the substrate. The 150 μm squares are the PEGDA hydrogel responsible for limiting protein and cell adhesion [7, 42, 46]. The reproducibility of such qualities is vital towards testing selective cell adhesion and growth as the next step and future medical applications. It was previously reported that the addition of benzophenone to make PDMS photo-patternable means the photomask needs to be spaced from the substrate by at least 80 μm. However, this limited the resolution of the features formed [33]. In this study we were able to demonstrate contact photolithography and thus higher pattern resolution without the space requirement. While the patterned area was limited to around 1 cm^2 with both the 5:1 and 20:1 samples, the channels were reproduced with the same accuracy and consistency throughout. Benzophenone exhibits an increasing imbibition

rate as the stiffness of PDMS decreases [57], which means the 20:1 PDMS has the highest penetration depth and fastest diffusion rate. While a favorable property for the polymerization of PEGDA, it also meant decreasing the priming time to 1 minute and longer exposure intervals to counteract thermal polymerization. Despite having a minimum of 25 μm channels in this study, we postulate the possibility of reaching lower measurements down to 10 μm.

In order to show that the patterned channels were well developed reaching the PDMS surface, protein adsorption was tested by covering the PDMS samples with albumin-fluorescein solution. As presented in **Figures 2.2b-d**, the green fluorescence in the channels shows patterned protein adhesion to the channels and not the PEGDA squares, signifying specific protein adsorption. Furthermore, this proves the absence of PEGDA aggregation at the bottom of the network, due to overexposure, that might have hindered protein attachment. This is vital to ensure cell adhesion which would be otherwise impeded by PEGDA residue in the channels.

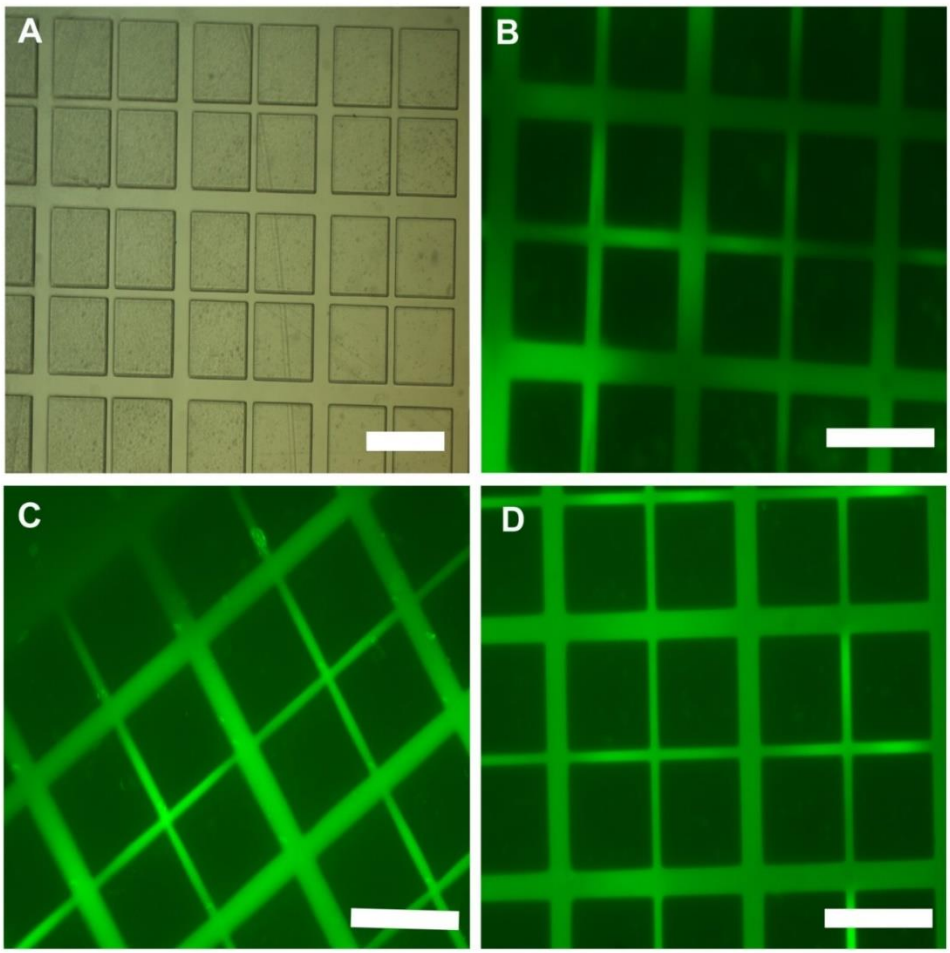

Figure 2.2: (A) Optical image of micropatterned 25 and 50 µm channels with 150 µm PEGDA squares on PDMS. Selective FITC-BSA adhesion to the channels signified by the green fluorescence in (B) 10:1 (C) 20:1 and (D) 5:1 PDMS samples (Scale bars = 200 µm)

While PDMS represents a more ideal substrate due the characteristics stated above and particularly being biocompatible and stable once patterned, it is very challenging to form features beyond grids. Complex features resulted in a big portion of the hydrogel settling on the photomask instead of the substrate with contact lithography. Exposure time and intensity had to also be altered constantly with inconsistent results. Since repeatability is a high priority for microfabrication to be applicable, this system still needs more optimization. Glass was therefore

used as a substitute in the second half of the experiments, since it showed more versatility in manipulating features over large areas without the need to introduce intervals for heat dissipation and being able to operate at low intensity and time.

Figure 2.3a shows channels ranging from 50 microns to 10 μm and precise grafting on a small scale. The total space occupied by the features was less than 0.5 cm and it showed promise for expanding the area occupied of the sample. **Figure 2.3b** shows the result of adding FITC-BSA to test selective adhesion. While fluorescence was mostly restricted to the channels, there were some patchy spots observed, which could indicate that there might be residual PEGDA in the channels. This observation was actually confirmed later as stated above, and resulted from initially adding 65 μL of solution to the substrate and having a 100 μm thick hydrogel which caused the channels to develop prior to reaching underlying the glass substrate. This was remedied by adding a smaller quantity of solution (20 μL) instead, and decreasing the distance between the light source and substrate to lower light scattering. **Figure 2.4c** indicates a 0.8 $inch^2$ glass substrate fully patterned with channels of 100, 50 and 25 μm widths are shown in **Figure 2.3d**. Precise fabrication was maintained while increasing the coverage area and more importantly getting consistent results with a fixed protocol. The explanation behind expanding the previous grid to such network like features is discussed in chapter 4 as it is meant to improve neural differentiation and test the effect of such topography on the properties of cells of the neural line.

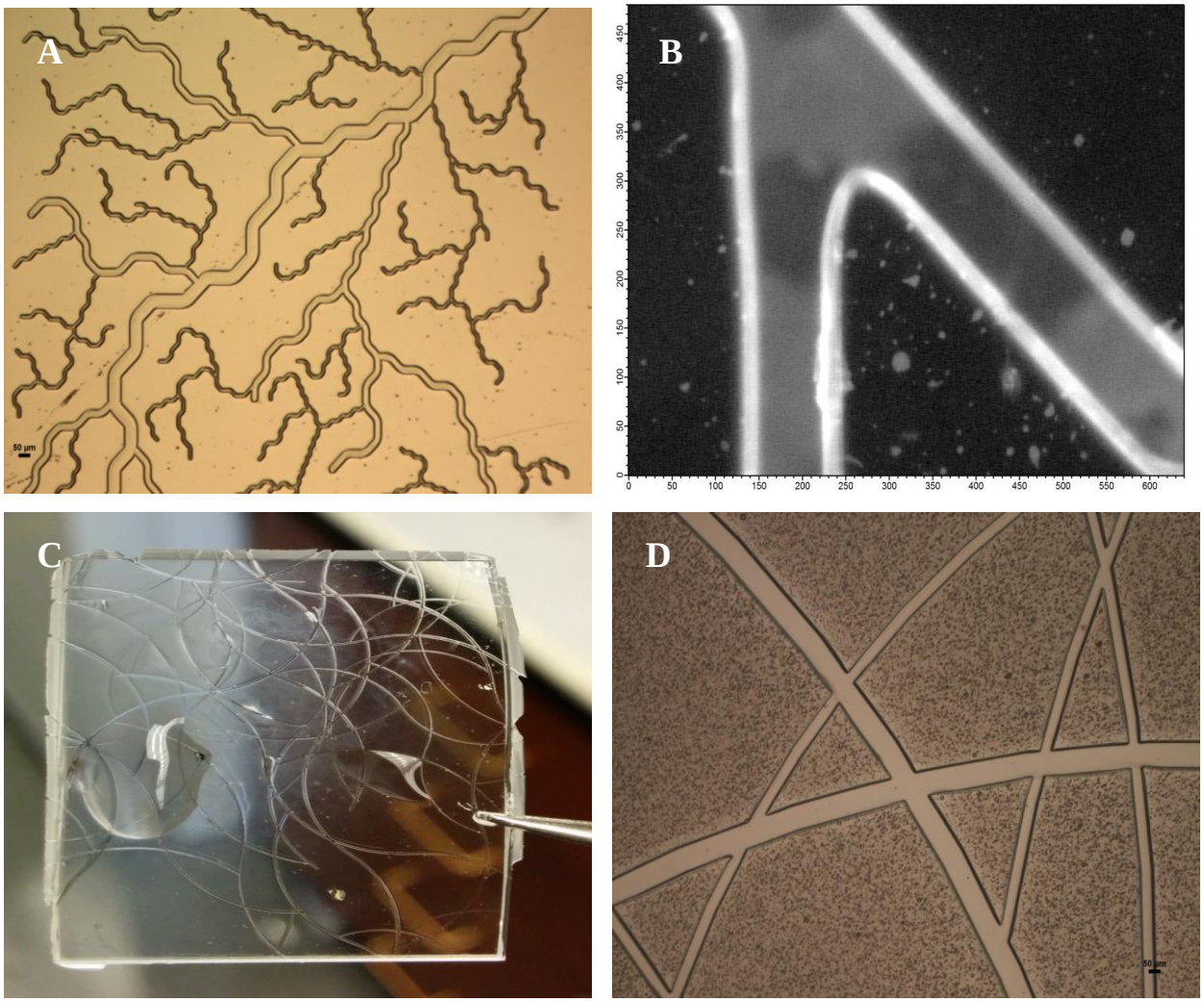

Figure 2.3: (a) Micropatterned glass with features ranging from 50 to 10 microns (b) Fluorescent protein adhesion to channels (c) Large scale patterning with high coverage (d) 4X image of the pattern

2.3 Optimization of micropatterning

2.3.1 Optimization of patterning on PDMS

Preliminary attempts to micropattern PDMS involved treating samples with oxygen plasma using the plasma cleaner PDC-32G (Harrick Plasma, USA) for 30 seconds to introduce hydroxyl groups on the surface. This was followed by 10 hours of TPM chemical vapor deposition. Upon

spin coating, the prepared PEGDA solution seemed to scatter off the surface even at speeds as low as 1000 rpm. The contact angle of water on the TPM treated PDMS was found to be 96°, which is almost the same as untreated PDMS indicating insufficient deposition. To resolve this issue, the first option was to increase oxygen plasma treatment duration to 5 minutes and perform silanization by immersing the samples in a solution containing 10-20 μg TPM per gram of perfluorooctane. The second investigated method involved immersion of the PDMS in 10 wt% benzophenone solution in acetone for 1 min, followed by adding reaction solution of PEGDA, sodium periodate and benzyl alcohol. The reported results for this method were limited to 100 μm [30], in addition to concern regarding acetone swelling up the PDMS. Upon examining the first choice and using heptane as an alternative to perfluorooctane, curvature in the samples was noticed afterwards and was hypothesized to be caused by heptane swelling up PDMS. On adding PEGDA solution and UV exposure, the hydrogel was found to be completely attached to the photomask with almost no adhesion to the PDMS substrate. 5 minutes of plasma treatment was found to be too long since the PDC-32G instrument works around a curve with 30-40 seconds being the ideal time for creating hydroxyl groups. The 30 seconds mark was already attempted with CVD TPM treatment method, which implied that the issue is mainly related to the TPM treatment. The liquid immersion technique uses heptane which has a swelling ratio of 1.34. Acetone on the other hand, which is used in the non-TPM treatment method involving benzyl alcohol and benzophenone, has a swelling ratio of 1.06 and time can be allowed for it dry [58].

PDMS slides were prepared and immersed in a 10 wt% benzophenone-acetone solution for 1 minute and rinsed with water. A reaction solution composing of 40 wt% PEGDA, 0.5 wt% benzyl alcohol and 0.5 mM sodium periodate in water was prepared. The mask was lowered on

top of the sample and UV exposure at 5% intensity for 3.5 seconds. The solution remained liquid however and did not from a hydrogel even at an intensity of 100% for 4 seconds. Adding 10 µL of Darocur resulted in the formation of a hydrogel but it did not attach to the PDMS. The following strategies were adopted to address this issue:

1. To improve benzophenone diffusion, the PDMS samples were divided and immersed for 5 minutes and overnight respectively.
2. A 35:65 (w/w) water/acetone mixture was used to prepare the benzophenone solution instead of pure acetone. An earlier study using poly(acrylic acid) instead of PEGDA indicated this to give the best pattern quality down to 5 µm [31].
3. 10 wt% PEGDA solution was prepared since the dilution might be helpful in facilitating entry of PEGDA monomers.

However, these trials did not show improvement in the results and polymerization could not be achieved even at 100% intensity for 15 seconds. Initial attempts with a 10% PEGDA solution resulted in the formation of a barely hydrated "cloudy" gel with much distorted features.

Increasing the composition to 40% however did result in the formation of a hydrogel after 5 minutes 15 seconds of exposure in a UV curing box (Loctite 7405), with the drawer slightly ajar for ventilation and avoiding heat polymerization. **Figure 2.4(a)** shows that even with these precautions, unstable attachment to the PDMS was observed. The hydrogel floated off after 24 hours incubation at 37 °C. This was a concern since, in order to sustain cell culture, patterns needed to be stable for at least 7 days. The composition of benzyl alcohol was increased to

rectify this. **Figure 2.4(b)** indicates PEGDA traces in the 100 μm channels due to overexposure which would inhibit cell adhesion in the channels and serve against specific micropatterning.

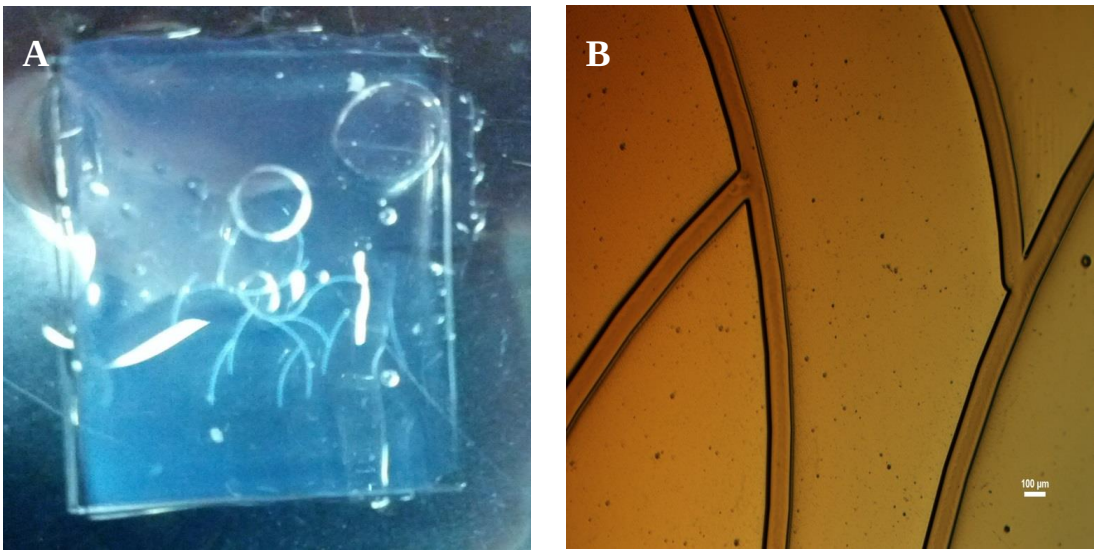

Figure 2.4: (a) Patterned PEGDA hydrogel on PDMS delaminates at 24 hours at 37°C (b) 4X brightfield view of the 100 μm channels with PEGDA traces in the channels

Benzyl alcohol in 1 ml of the monomer solution was increased to 50 μL (5 wt %) to improve hydrogel attachment. Following these trials, it was concluded that the UV curing box was not suitable for controlling heat polymerization as it allowed limited manipulation to the protocol due to a fixed intensity and light source distance. The UV spot lamp was reverted back to with a higher intensity (75%) used to ensure polymerization. Several trials were attempted with different exposure times and intervals to dissipate heat until settling for the protocols stated in the previous section with respect to the PDMS ratio and stiffness. However, it must be noted that these steps were set for the simpler grid structures and features over smaller areas in comparison to the substrate (as seen in **Figure 2.4**). This therefore led to some inconsistencies with different trials. However, successful attempts resulted in precise features down to 10 μm with accurate

protein attachment (**Figure 2.5**). Furthermore, the hydrogel and features were stable when incubated for 7 days in 37 °C and months at room temperature.

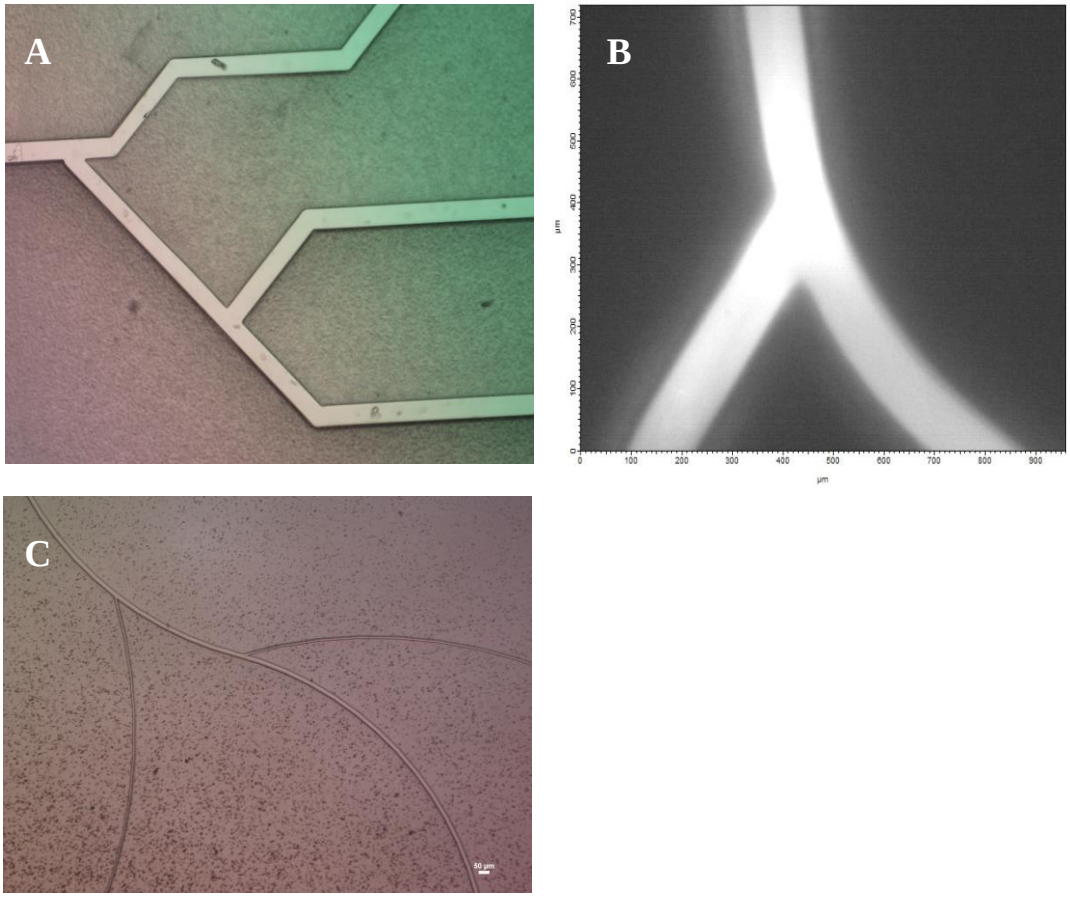

Figure 2.5:(a) 100 micron channels reaching PDMS and a stable hydrogel (b) FITC-BSA tests shows specific protein adhesion (c) features down to 10 microns

2.3.2 Optimization of patterning on glass

As PDMS resulted in inconsistent results, we investigated glass surfaces for studying the cell culture as a function of network architectures. Initially TPM treatment resulted in “blotches” on the glass slides due to prolonged vapor deposition in the desiccator at -0.2 bars for about 16

hours. Upon repetition the "blotching" issue was resolved by reducing the amount of TPM used from 500 µL to 100 µL per every 3 slides and limiting vapor deposition to 12 hours. Slow deposition of TPM was also ensured to avoid splashing that might result in buildup of multilayers. Spin coating was first used to obtain a thin, uniform PEGDA layer to be patterned. Glass slides were spin coated with undiluted PEGDA and Darocur mixture to optimize the dispensed amount and spin speed which would result in a uniform, thin film. The attempts ranged from around 20 µL of PEG mix at 2500 RPM to 40 µL at 4500 RPM. The square-like geometry of the substrate can face "increased friction with air at the periphery, resulting in increased evaporation rate which cause dry skin to form at the corners and impeding fluid flow". To remedy this issue, dynamic dispense was tried where the glass slide is rotated at a slow speed of 500 RPM. This is followed by the acceleration step at 1500-6000 RPM to thin the film. The solution was also be diluted with ~40 wt% water. The amount dispensed on the substrate was kept within the 20-40 µL limit. The 2-step spin coating process used with photoresist was first attempted, followed by a series of 1-step attempts. Optimal speed was 1000 rpm for 90 seconds at an acceleration of 50 r/s^2, covering the most area. However, this still did not provide high enough coverage of the substrate nor uniformity. It should be noted that all attempts showed spreading of the PEGDA solution in mainly the diagonal direction.

An alternative method was experimented next that was potentially more effective and less time consuming than spin coating, especially owing to the relatively lower viscosity of PEGDA compared to SU8-2050 photoresist. This option involved cutting a 170 µm thick plastic coverslip into two pieces to be used as spacers. Upon placing them on the sides of the TPM coated glass, a micropipette was used to inject the PEGDA solution. A full cover slip is then placed on top

allowing the solution to spread uniformly across the substrate through capillary action forming a 170 µm thick film. The coverslip is then removed before exposure since it might distort the pattern being photografted.

The patterns obtained were left in a hydrated environment for a week. Upon re-checking it the hydrogels were found to be still intact which demonstrated effective TPM treatment. However, when examined under the microscope appeared to include irregularity and shrinkage in width, blockage of channels and not being deep enough to reach the glass surface, as seen in **Figure 2.6(a)**. The thickness of the PEGDA hydrogel was then reduced to 100 µm by removing the spacers and reducing the volume of PEGDA solution added from 109 µL to 65 µL. Exposure time was increased to 3 seconds and the UV light source was set to 2 inches above the substrate. An issue with air bubbles was initially encountered but was resolved on the following trial by slowly lowering the cover slip on the sample. This relieved any previous blockage and channels were consistently visible, appearing to be deeper as shown in **Figure 2.6(b)**. Feature shrinkage however continued (for instance 100 µm on the photomask end up as 40 µm).

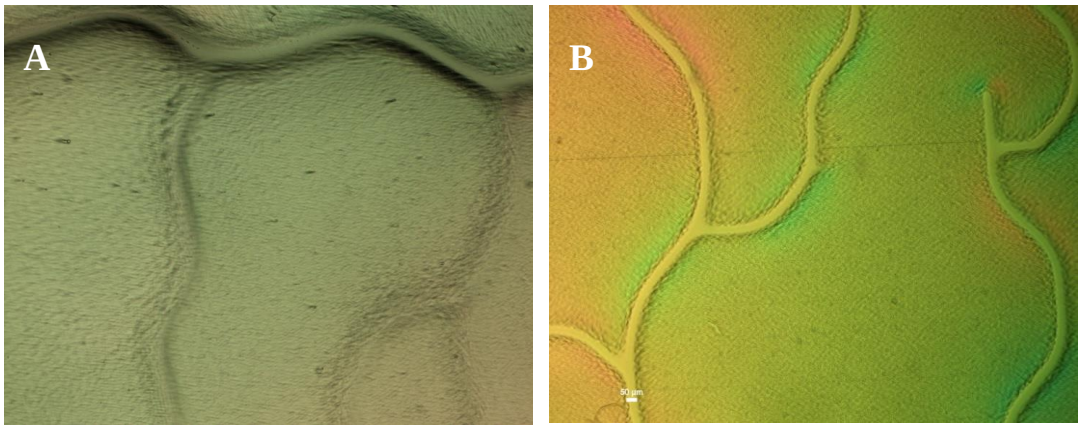

Figure 2.6: (a) Patterns are irregular in width with blockage of channels and not reaching the glass surface (b) Improved results with a thinner PEGDA hydrogel but shrinkage remains apparent.

In order to obtain the lower width channels the following trials were performed and focused on three patterns each of widths 50 µm, 25 µm and 10 µm.

1) 50 µm hydrogel thickness with 3 seconds exposure under 5% intensity
2) 50 µm hydrogel thickness with 2.2 seconds exposure under 5% intensity
3) 50 µm thickness with 1.5 seconds exposure under 5% intensity
4) 30 µm thickness with 1 second exposure under 5% intensity
5) 100 µm thickness with 2 seconds exposure under 5% intensity

While run 3 and 4 resulted in underexposure and inability to form a hydrogel, the rest of the runs involved somewhat similar results with very little change. The main issue to be resolved was the shrinkage of the patterns. A negative test mask was used with a 40% PEGDA solution instead.

Upon preparing the glass slides, the first step taken to solve the shrinkage issue was to remove any suspension of the mask and place it directly on the cover slip. Upon repetition under the conditions of 5% intensity for 3 seconds and a 100 µm thick hydrogel, improvement was observed (56.5 µm wide pattern compared to 40 µm earlier). To get a better understanding of the reason behind the shrinkage, a dark field mask was used instead, while keeping the same parameters to track different widths ranging from 100 µm to 1 µm. Initially, the 100 and 50 µm lines were the only ones obtainable with a lot of merging and haziness involved between the projections as seen in **Figure 2.7(a)**. To solve this issue the cover slip was removed and contact lithography was attempted. Upon applying the PEGDA solution to substrate, the mask was place on top to create the "uniform" layer. This showed noticeable improvement in the results, as indicated in **Figure 2.7(b)** and proved that the cover slip was the main cause since it absorbed

UV light, added more space between the solution and the mask and introduced distortions. While it solved the clarity issue, there seemed to be signs of underexposure, insufficient height and smaller widths for the 50 and 25 µm lines. Therefore, this last trial involved exposure for 4 seconds instead of 3 and increasing the amount of PEGDA solution added from 28 µL to 35 µL. This again showed further enhancement and helped achieve more defined feature with more detail (**Figures 2.7 (c)** and **2.7 (d)**). More optimization was still required to improve the pattern clarity and be able to reach widths as low as 10-15 µm, the next trials involved reverting back to the bright field mask features since they are the primary objective. This lead to the result previously stated in **Figure 2.3(a)**.

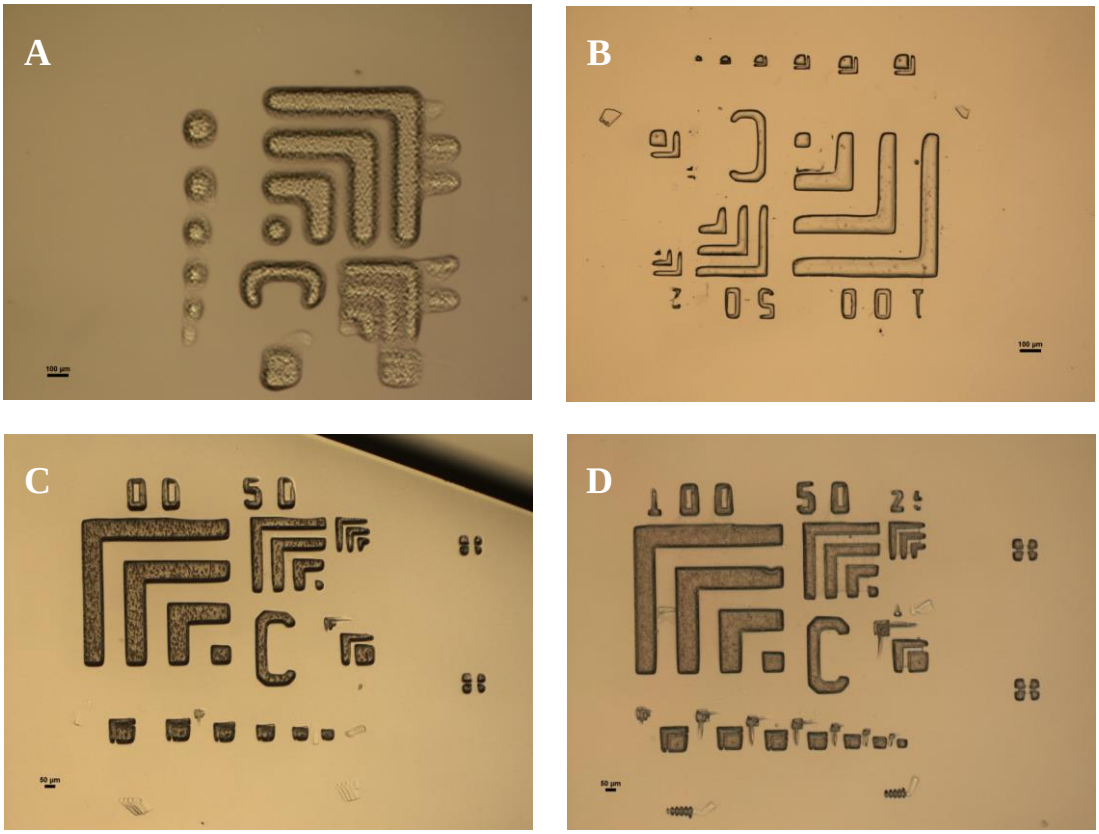

Figure 2.7: Darkfield photomask test shows (a) hazy, undefined projections with the coverslip (b) improved features using contact lithography (c) and (d) high pattern clarity down to 10-15 µm.

To check specific protein attachment to the channels obtained from the brightfield photomask features in **Figure 2.3(a)**, the glass substrate was incubated in a 1mg/ml BSA solution in 1X PBS at 37 °C overnight. The PEGDA hydrogel detached and therefore exhibited instability at 37 °C for a long enough period that would allow testing cells. This observation is again confirmed in Chapter 4 with more detail regarding specific cell attachment. The PEGDA concentration was increased to 60 vol. % as a remedy to enhance the network cross-linking, increase the mechanical modulus and decrease swelling ratio with the temperature. While overnight incubation showed how the stability of the hydrogel could be improved, it resulted in high background fluorescence. The sample was therefore immersed for 30 minutes (**Figure 2.3(b)**). This indicated a positive result of protein aggregation and attachment inside the channels. **Figure 2.8** also shows how channels that may appear clear and well defined, do not necessarily reach the glass substrate.

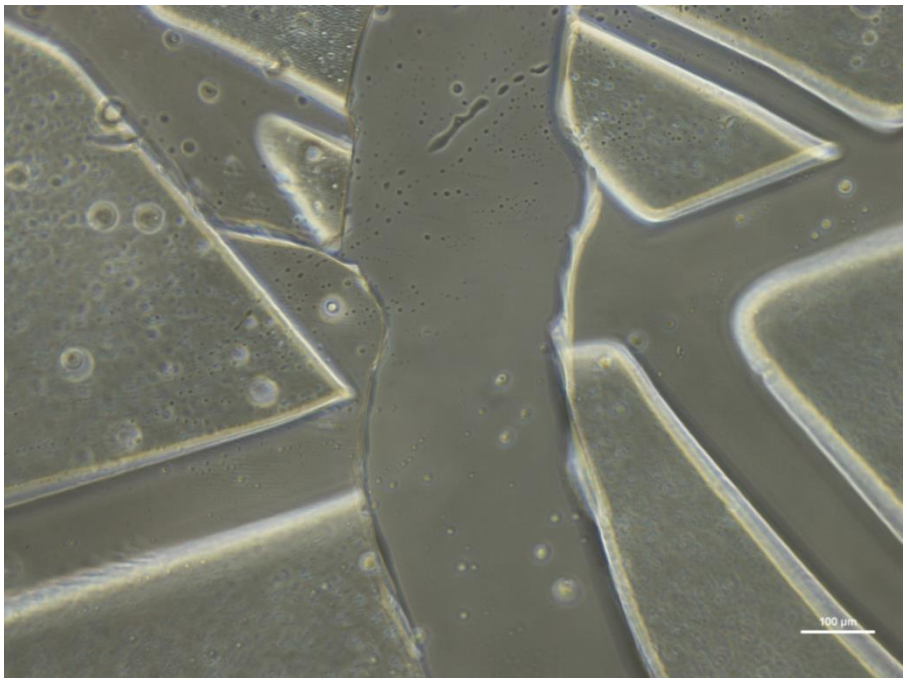

Figure 2.8: Micropatterned channels appear to have edges rather than empty space indicating they have a layer of PEGDA at the bottom.

2.4. Conclusions

In this chapter, the formation of a stable and long-lasting PEGDA hydrogel photo-grafted on PDMS and glass surfaces was shown that maintains function in specifically resisting protein adhesion. Increasing the benzyl alcohol concentration in monomer solution promoted hydrogel attachment and decreasing benzophenone treatment time with the introduction of time intervals during UV exposure helped counteract thermal polymerization. Such measures lead to achieving specific, high density protein adhesion on PDMS that can be uniformly micropatterned up to an area of 1 inch^2. While consistency was an issue with more complex features beyond a simpler grid pattern in terms of exposure parameters, once obtained though the hydrogel was as stable over large areas with precise features and provided a platform for testing cell adhesion next. Glass offered more regularity and versatility when it came to patterning despite being a less preferred substrate. Features down to 10 μm were obtained and optimized to ensure the channels are reaching the glass by reducing the hydrogel thickness.

Chapter 3: Cell culture on micropatterned substrates

3.1. Introduction

Once the micropatterned PDMS and glass substrates are formed with resistance to non-specific protein adhesion as shown in the previous chapter, investigating cell adhesion and proliferation is the next step. This serves as the main purpose behind the microfabrication and is directed at providing clear insight over the applicability of PDMS as a biocompatible substrate in future aspects. The surface of PDMS is highly hydrophobic (contact angle: 105°) which tends to result in the non-specific adsorption of proteins and other biologically significant biomolecules required for cell attachment and growth [59, 60] . This is also explained by the low surface energy between water and PDMS (20 dynes/cm) which means less cell adhesion compared to substrates with suitable, intermediate surface energy (57 dynes/cm) [32]. Surface modification is therefore often required for effective application of PDMS and to improve its ability to promote cell attachment. For instance, coating it with fibronectin has been proven to be suitable for culturing fibroblasts at growth rates comparable to polystyrene and glass, despite lower initial cell attachment. Recent findings show that fibronectin improved the fibroblast adhesion by 32% over untreated surfaces [53].

In addition to architecture of the micropatterning, another parameter of interest was the underlying substrate stiffness (a feature that makes PDMS attractive in the first place). Cell behavior in terms of proliferation, spreading and attachment can be regulated by altering the

stiffness of the substrate. Acting as the *in vitro* extra cellular matrix (ECM), its mechanical properties influence the chemical and physical cues responsible for cell fate. Different cell types vary in terms of the adhesion and proliferation to the change in stiffness of the substrate. For instance, vascular smooth muscle cells have been found neural progenitor cells were found to favor neuron and astrocyte differentiation on softer surfaces but oligodendrocyte differentiation on stiffer substrates [61]. This indicates that such change in the mechanical properties of the substrate can also influence lineage specification. Further, human embryonic stem cells proliferation has been previously shown to be affected by varying the stiffness across 10:1, 20:1 and 40:1 PDMS, while cell spreading and attachment still remained similar [53]. Fibronectin adsorption and therefore adhesion of fibroblasts has also been stated to respond to different PDMS substrates. While the amount of adsorption was practically the same, the exposure of cell-binding motif differed based on the nanoscale surface stiffness and therefore reflected on the cell adhesion behavior [62]. So far, previous studies involved examining the effect of stiffness change on un-patterned PDMS [34, 53, 62] and for the sake of optimizing cell micropatterning for different cell types, it is vital to test its impact as an additional cue.

3.2 Materials and methods

3T3 mice fibroblasts and human dermal fibroblasts were used to test cell adhesion and cell growth. 4',6-diamidino-2-phenylindole (DAPI) and Alexa Fluor Phalloidin 488 were acquired from Life Technologies (Grand Island, NY, USA). Micropatterned PDMS samples were stored in 1X PBS solution and sterilized by UV exposure for 30 minutes (less than 0.01 W/cm^2). To promote cell attachment, 10:1 samples were subsequently immersed in 3 ml of 6 μg/ml

fibronectin solution for one hour prior to cell culture, while 20:1 and 5:1 substrates had 10 μg/ml. In order to confine adhesion to the samples, the bottom of the tissue culture plates was coated with 1% agarose prior to cell culture. The gel was prepared by adding 0.1 g of agarose (BioExpress, UT) to 10 ml of diluted 1X Tris-borate-EDTA (TBE) (Bio-Rad Laboratories) buffer and autoclaving it using a Castle 133LS vacuum steam sterilizer (Getinge, NY) for 20 minutes at 121 °C.

3T3 mice fibroblasts were cultured at 37 °C in 5% humidified environment in Dulbecco's modified eagle's medium (DMEM) with 10% fetal bovine serum . Upon reaching ~90% confluence in four days, the cells were trypsinized (0.25% trypsin solution) and passaged at a density of $5x10^4$ cells per PDMS sample. Human dermal fibroblasts (HDFs) were maintained in minimum essential medium supplemented with 2 mM l-glutamine, 1% penicillin/ streptomycin, 10% fetal bovine serum, amino acids, sodium pyruvate and vitamins [63]. Cells were cultured on the 20:1 and 5:1 samples at $7x10^4$ cells per sample. Following 6 days of cell culture the samples were fixed by adding 4% paraformaldehyde solution for 30 minutes. Phalloidin 488 was added as a cytoskeletal stain and DAPI as a nuclear stain for 30 minutes each. Samples were washed for 5 minutes three times using PBS wash buffer following each step.

3.3. Results and discussion

A major concern for cell adhesion is presence of the photoinitiator benzophenone after UV polymerization since it is known to be toxic for cells and could introduce problems for biological applications [33, 64]. It was observed that increasing the benzophenone beyond 2 minutes

reintroduced the thermal polymerization issue and decreased the stability of the hydrogel which turned cloudy. It was previously suggested to immerse the samples in acetone for 5 minutes in order to remove the benzophenone [30]. However, such treatment resulted in the hydrogel drying and delaminating instantly, which lead to use of 50 wt% acetone solution in water. ATR-IR spectroscopy was conducted to verify the extent of benzophenone removal from PDMS surface prior to cell culture. **Figure 3.1** shows that benzophenone is still present in the samples whether they were rinsed in the solution or not. This is exhibited by the peak near 3000 cm^{-1} representing the C-H stretching of an aromatic ring and the carbonyl group (bridging the two phenyl rings) peak at 1720 cm^{-1}. Upon rinsing the samples with the 50 wt% acetone solution and storing them in water overnight, an attenuation of these peaks shows the benzophenone is washed away.

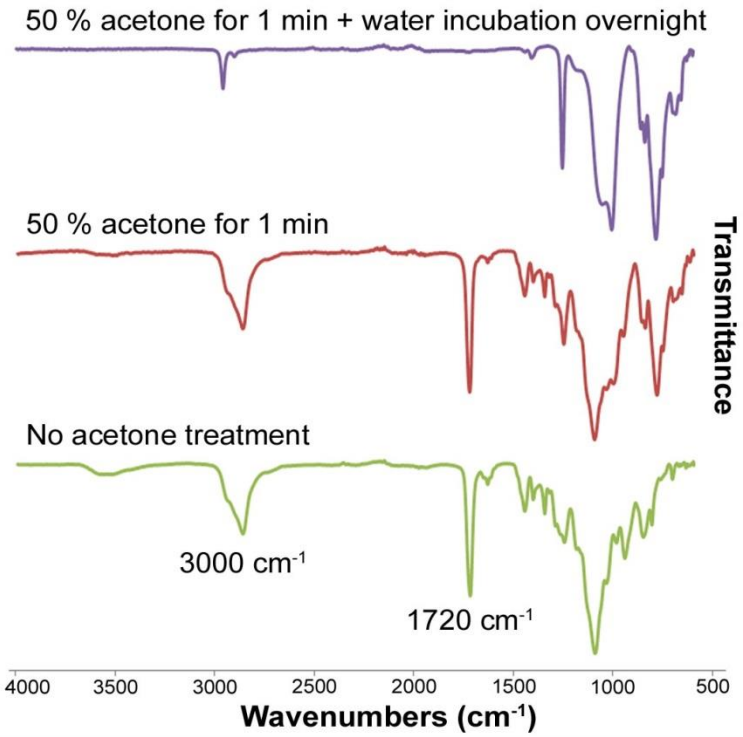

Figure 3.1: Attenuation of 3000 and 1720 cm-1 peaks indicates benzophenone is washed away up rinsing PDMS with 50 wt% acetone solution for 1 minute and overnight incubation in water.

To demonstrate patterned cell adhesion and growth, 3T3 mice fibroblasts were cultured at a density of $5x10^4$ cells/well on the fibronectin coated 10:1 PDMS sample. Since native PDMS does not promote cell attachment due to its high hydrophobicity [59, 60] coating the PDMS with fibronectin allowed cell adhesion and proliferation. After 6 days the PEGDA hydrogel showed no cell attachment, which was limited to the channels as required for specific cell patterning. The cells were shown to be fully proliferated and interconnected at high density throughout the pattern to form a network as illustrated in **Figure 3.2(a)**. The 50 μm channels showed the aggregation of several cells compared to the smaller 25 μm channels which had one or two cells aligned. This indicated that not only the adhesion was confined to the PDMS channels but that they responded to spatial cues and distributed accordingly rather than simply accumulating in larger areas. In order to demonstrate the successful micropatterning on the 25 and 50 μm channels, the cells were fixed using 4% paraformaldehyde in PBS and stained with both DAPI and Phalloidin. **Figure 3.2(b)** shows the cell nuclei and cytoskeleton overlaid.

To ensure the future applicability of micropatterned PDMS in fields such as tissue engineering, testing human cells is a vital step to ensure consistency. HDFs were cultured on 5:1 and 20:1 PDMS substrates to also monitor the effect of stiffness and improve the cell to surface interactions through better mimicking of the tissue microenvironment. A previous study indicated substantially higher adhesion density of NIH3T3 mouse fibroblasts 20:1 PDMS than the stiffer options. The reasoning was that despite being less stiff on the macroscale, 20:1 PDMS exhibited maximum stiffness on the nanoscale and exposed cell-binding motifs [62]. On the other hand, a different study found transformed 3T3 fibroblasts to grow at similar rates on PDMS irrespective of stiffness [34] . **Figures 3.2(c) and 3.2 (d)** show that 20:1 and 5:1 PDMS

maintained precise cell adhesion to the channels but at lower densities compared to 10:1. While having less available surface area due to the 1 cm^2 limitations could justify the density difference, the morphology and slow proliferation of the adhered cells is an indication that stiffness is the major contributor. This is further supported by **Figure 2.2** which shows consistent fidelity of the features. Favoring normal PDMS over 20:1 supports the claim that fibroblasts migrate preferentially to stiffer substrates and exhibit stronger traction forces [65]. Even though 5:1 PDMS shows mildly higher proliferation and attachment than 20:1 PDMS, it does not follow the previous claim when compared to normal PDMS. Such discrepancy could be attributed to the optimal cross-linking density of 10:1 PDMS and the higher amount of un-crosslinked components when increasing the crosslinker or based beyond the normal ratio [34]. These components can be either mobile affecting the nutrients in growth media or stationary on the PDMS surface influencing cell attachment and growth.

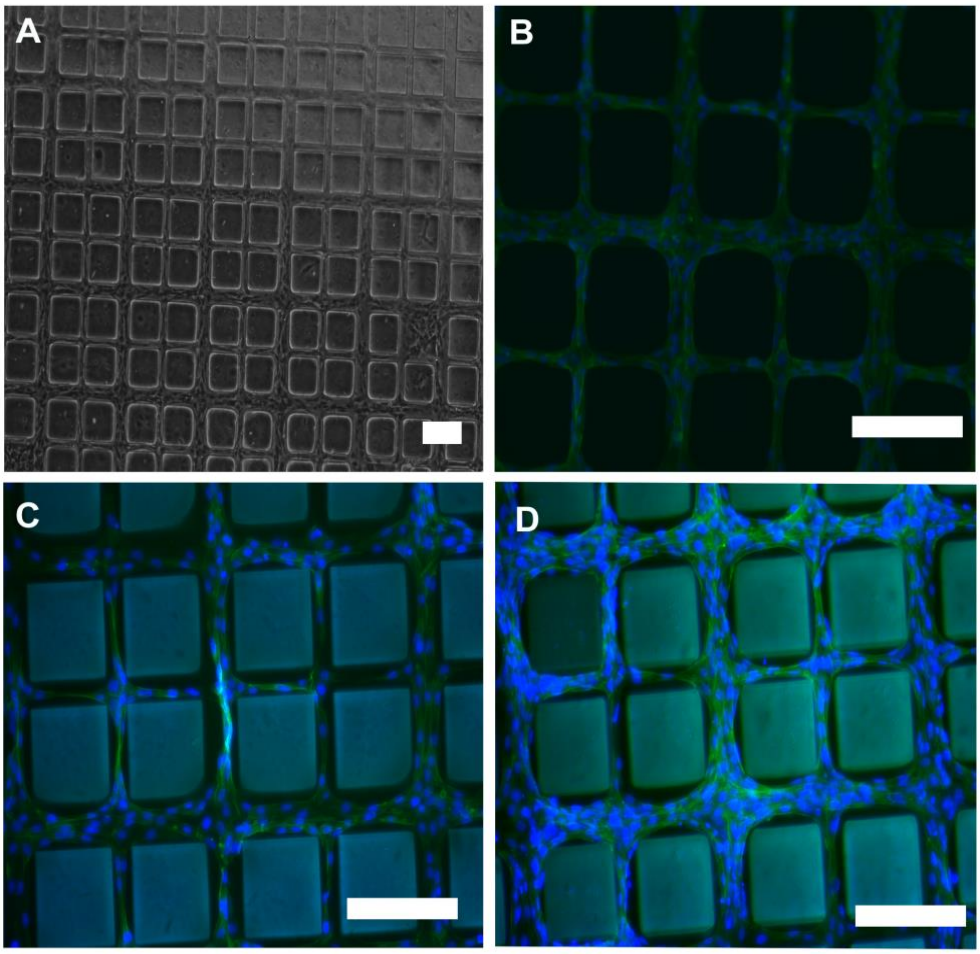

Figure 3.2: (a) A brightfield optical micrograph of the fixed 3T3 mice fibroblasts on 10:1 PDMS after 6 days forming an interconnected network around the PEGDA 150 µm squares. Phalloidin and DAPI stained cells shown through a 10X objective lens with the nuclei and cytoskeleton overlaid on (b) 10:1 PDMS (c) 20:1 PDMS and (d) 5:1 PDMS (scale bars = 200 µm)

3.4 Optimization of cell culture on patterned substrates

On culturing human dermal fibroblasts on 20:1 PDMS for three days, no traces of cell adhesion were found on the two PDMS samples. Despite following the same protocol as the previously obtained mouse 3T3 fibroblasts on 10:1 PDMS, the HDFs did not show attachment or proliferation and continued to float, maintaining a circular shape as shown in **Figure 3.3(a)**.

These same cells however showed healthy proliferation on a tissue culture plate after 3 days (**Figure 3.3(b)**).

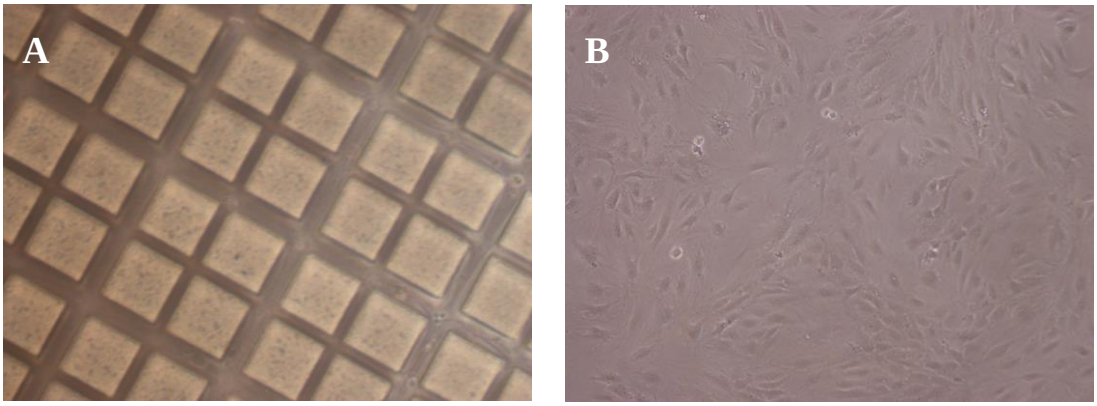

Figure 3.3: After culturing HDFs for 3 days (a) 20:1 PDMS showed almost no attachment or proliferation (b) TCP exhibited healthy HDF growth and spreading at high density.

After 6 days, a few cells showed proliferation restricted to 50 μm channels as seen in **Figure 3.4(a)**. Staining the cells with DAPI and phalloidin in **Figure 3.4(b)** confirmed the lack of growth and spreading. While the images showed some attachment and growth of human dermal fibroblasts in the channels, a higher density was still needed for proper comparison with the 10:1 PDMS. An extra step was added to the preparation of the hydrogel which involved immersing the sample in a 50 wt. % acetone solution in water for 1 minute. This was be followed by overnight incubation in water before cell culture and is supported by findings in the previous section and **Figure 3.1** to remove traces of benzophenone which might be toxic. Despite not appearing to be an issue with 10:1 PDMS, the stiffness of the samples has been reported to influence benzophenone diffusivity with softer PDMS exhibiting a higher rate [57]. 5:1 PDMS was also attempted as a possible alternative for comparison. HDFs where again passaged at a density of 50,000 cells and followed by DAPI and Phalloidin staining. **Figures 3.4(c) and (d)**

illustrate an observed higher density of attached cells on day 6 but with most of them not exhibiting healthy spreading characterized by HDFs. Since attachment was a concern with both PDMS ratios, we decided to increase the fibronectin concentration added to 10 µg/ml. 1% agarose gel was also introduced at this stage to coat the bottom of the wells and help limit cell migration to the sample, especially with PDMS being light and likely to float close the surface. The results were those presented previously in **Figure 3.2** and provided enough cell adhesion and proliferation for conducting an assessment next to 10:1 PDMS.

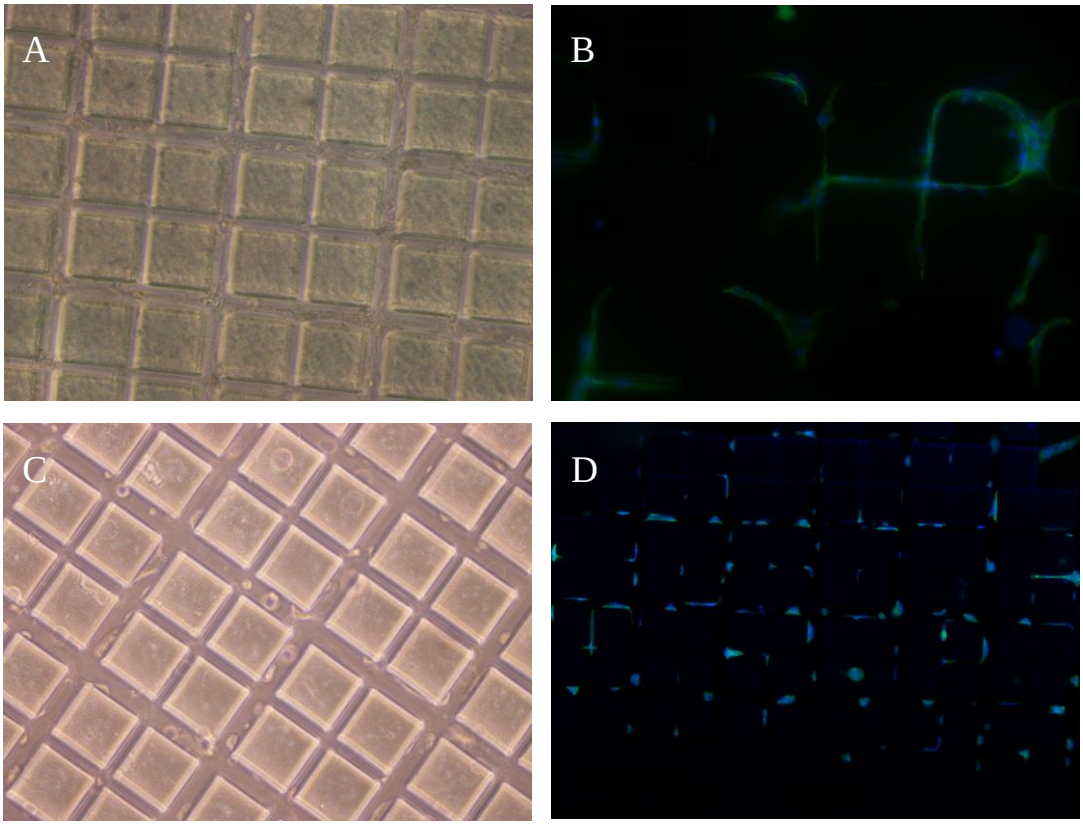

Figure 3.4: HDFs cultured for 6 days on (a) 20:1 PDMS with limited attachment and proliferation and (b) 5:1 PDMS showed higher density of cells but very low spreading. (c) and (d) involved DAPI and Phalloidin staining to illustrate the results.

3.4. Conclusions

The effect of altering the mechanical properties of the patterned substrate, through stiffness, on cell behavior was examined on 10:1, 20:1 and 5:1 PDMS samples. Controlled cell adhesion and proliferation was achieved for all three ratios with the cells migrating specifically to the PDMS channels surrounded by PEGDA. Normal or 10:1 PDMS, which is also the favored composition by the manufacturer, was found to be optimal in terms of stiffness and uncrosslinked components for growing fibroblasts on micropatterned regions. Furthermore, 50 wt% acetone treatment was introduced following UV polymerization to remove traces of benzophenone which might be toxic to cells. This study shows potential to further increase the micropatterning areas while reaching smaller widths on the microscale. More complex features can also be adapted that mimic the *in vivo* microenvironment and be used for directing cells into specific lineages and controlling their fate.

Chapter 4: Cell culture on 'open network' micropatterns for neuronal propagation

4.1. Introduction

Neuronal systems are delicate and prone to various disorders and diseases such as injury, Parkinson's disease, Alzheimer's disease and ischemia. Possessing limited regenerative abilities, neurons can lose functionality but rarely recover naturally. This has necessitated *in vitro* models to accurately investigate such disorders, as well as to help in developing regenerative therapies or nerve replacements as implants [66, 67]. However, relevance to the *in vivo* scenario and developing functionally mature neurons has been a concern which still hinders progress in this field [68]. Randomly cultured *in vitro* neurons tend to disrupt electrical signals which are highly structured in a brain [69]. Interconnected, organized control of neuronal cells to mimic the intracellular architecture and environment could provide better insight. Micropatterning the cells and using geometric cues to induce neuronal differentiation and reduce the amount of biochemical stimuli has therefore been an important avenue for investigation.

Various methods which use microcontact printing, gratings and nanofiber matrices have been attempted and found to increase neural differentiation in terms of rate, morphology and expression of biological markers such as NeuN, GAP43 and β3- tubulin [18, 19, 70]. Some studies have shown topographic control to promote neuronal differentiation from stem cells or cells such as the human neuroblastoma cell line SH-SY5Y, without the need for soluble

induction factors such retinoic acid (RA), nerve growth factor (NGF) and brain derived neurotrophic factor (BDNF) [66, 71]. However, to date, such cells have typically been grown in straight, parallel channels. While, these regular geometric architectures illustrate neurite extension and tangential migration of neurons along the lines; features that are vital for neurite outgrowth [70], they do not adequately recapitulate the natural architectures of neurons. Therefore, the next step would be to improve these patterns into 'open networks' and incorporate them with biochemical factors. Here, the term 'open network' refers to features that are mostly interconnected throughout the scaffold and not aligned, with no clear beginning or end. Thus all the cells cultured on the substrate would interact and hopefully improve the efficiency of signal transmission since there is no segregation. Based on the techniques demonstrated in the prior chapters, the focus of this part of the study was to fabricate open networks and specifically focus on neuronal cell lines and their culture. To simulate the formation of such networks, photolithography was used to form varying degrees of branched architectures that are more complex than simple geometric patterns. SH-SY5Y cells were then cultured on these branched open networks to investigate the effect of the underlying architecture.

SH-SY5Y cells normally lack the morphology and expression of markers and proteins which are specific to mature neurons. Upon differentiation, they stop continuously proliferating and induce phenotypes depending on the agents used to promote it. For instance, retinoic acid (RA) alone results in a cholinergic phenotype, but when coupled with other agents can produce dopaminergic neuronal differentiation which is more required for Parkinson's disease related research [72]. They have also recently shown promise in exhibiting characteristics of mature neurons through the inclusion of topography with such agents. While neural progenitors and

stem cells represent more promise for direct application in regenerative medicine, SH-SY5Y cells have the potential to highly improve *in vitro* models of neurodegenerative diseases, especially with recent work introducing several cues that enhance their neural differentiation [67, 68, 70-72]. Consequently, these cells were selected for to study the effects of architecture and micropatterning.

4.2. Materials and methods

Human neuroblastoma cells (SH-SY5Y) were maintained at 37 °C in 5% CO_2 humidified environment in Dulbecco's modified eagle's medium (DMEM) supplemented with 2 mM l-glutamine, 1% penicillin/streptomycin, 10% fetal bovine serum, 110 mg/L sodium pyruvate and 2.5 g/L d-glucose (Gibco, Grand Island, USA) . Media was changed every two days and upon reaching ~90% confluence, the cells were trypsinized (0.05% trypsin solution) and passaged at a density of $6x10^4$ cells. The following substrates were used: 60 wt% PEGDA patterned on glass, a glass control and a TCP control. The bottoms of wells were coated with 1% agarose for the patterned glass sample and glass control to restrict cell adhesion to them. Cells were allowed to attach and proliferate for two days before inducing differentiation using RA (10 μM). Neurite lengths and cell body widths were also measured after differentiation by taking images on Days 5 and 6 with the aid of NIS-Elements microscope imaging software for the measurements. The full cell lengths were also taken from one end of a neurite to the other. The criteria for determining neurites was based on a protocol previously published which regarded points with widths less than 3.85 μm to be neurites [67, 71]. From two repeated cell cultures, 74 cells and neurites were measured; inside the channels of the PEGDA sample and in open space with

regard to the TCP and glass controls. At least two images were used for each condition. Cells were considered differentiated when the neurite length was found to be more than the cell body [70]. Statistical significance among the data was evaluated using single factor ANOVA.

To test the effect of surface architecture, a low reflective chrome photomask was fabricated includes four networks with the varying surface areas of 5, 7, 10 and 15% as seen in **Figure 4.1**. This allows differing spaces for the SH-SY5Y cells to attach, and better observe the effect the branched pattern (‘open network’) on cell proliferation or differentiation. Varying the available area and branching allows us to study the influence on differentiation of neuroblastoma cells to those with resemblance to adult neurons, and whether any of them show noticeable improvements over the rest. The 15% area network is the one presented in this study and was primarily incorporated to ensure as much as coverage as possible. The patterned glass substrate is the one previously shown in **Figures 2.3 (c & d).**

Figure 4.1: 5-inch low reflective chrome mask including four networks occupying 5, 7, 10 and 15% in surface are coverage.

4.3. Results and discussion

On passaging the SH-SY5Y cells on micropatterned glass and maintaining them for two days, the cells adhered specifically to the 25 and 50 μm channels as shown in **Figure 4.2(a)**. The 60% PEGDA hydrogel succeeded in resisting cell attachment between the patterns and maintaining spatial localization compared to the 40% PEGDA hydrogel shown in the optimization section. **Figure 4.2(b)** indicates that even prior to differentiation, the cells align along the channels and elongate inside the 25 μm features which constrain them. Thus the topography was already starting to a play a role in aiding neurite growth. Such an observation is consistent with studies which have already exhibited that lanes with even smaller widths actually induce neurite outgrowth and extension past the use of soluble factors alone [66, 71]. Adding RA further enhanced differentiation and as seen in in **Figure 4.2(c).** Cells started developing neurites with the cell body shrinking down in width and aligning with the 50 μm rather than the more random orientation that was still observed in **Figure 4.2(b).** Since the architecture is an 'open network', it implies that the cells interact throughout the scaffold forming a higher surface area for signal transmission and is how neurons are oriented *in vivo* rather than separate channels. **Figure 4.2(d)** illustrates the high density of neurites extending for the cells to establish a connection at the intersection of various channels and adapt by migrating along the tangent without stepping over the PEGDA hydrogel. It should be noted that the cells continued to proliferate as their numbers on Day 6, in **Figure 4.2(d)**, were clearly higher than before differentiation and did not stop dividing. This means they might require additional soluble factors in the future that would increase the efficiency of differentiation. RA would be a pretreatment for one week and the cells

will be then cultured in media containing - Brain derived neurotrophic factor (50 ng/ml), Neuregulin B1 (10 ng/ml), Nerve Growth Factor (10 ng/ml) and Vitamin D3 (24 nM).

To justify the need for patterning the SH-SY5Y cells in open architectures over un-patterned surfaces, the results were compared to a TCP and glass controls. **Figure 4.3** shows images taken on day 5 and while cells clearly developed neurites in all three cases, the channels forced the cell body to elongate and appear narrower in width. Rather than the random positioning of the cells and neurites on the controls, they were aligned in the channels. The neurites were mostly in tangent to the lane instead of spreading out horizontally, resulting in an organized parallel pattern of the connected cells throughout the network.

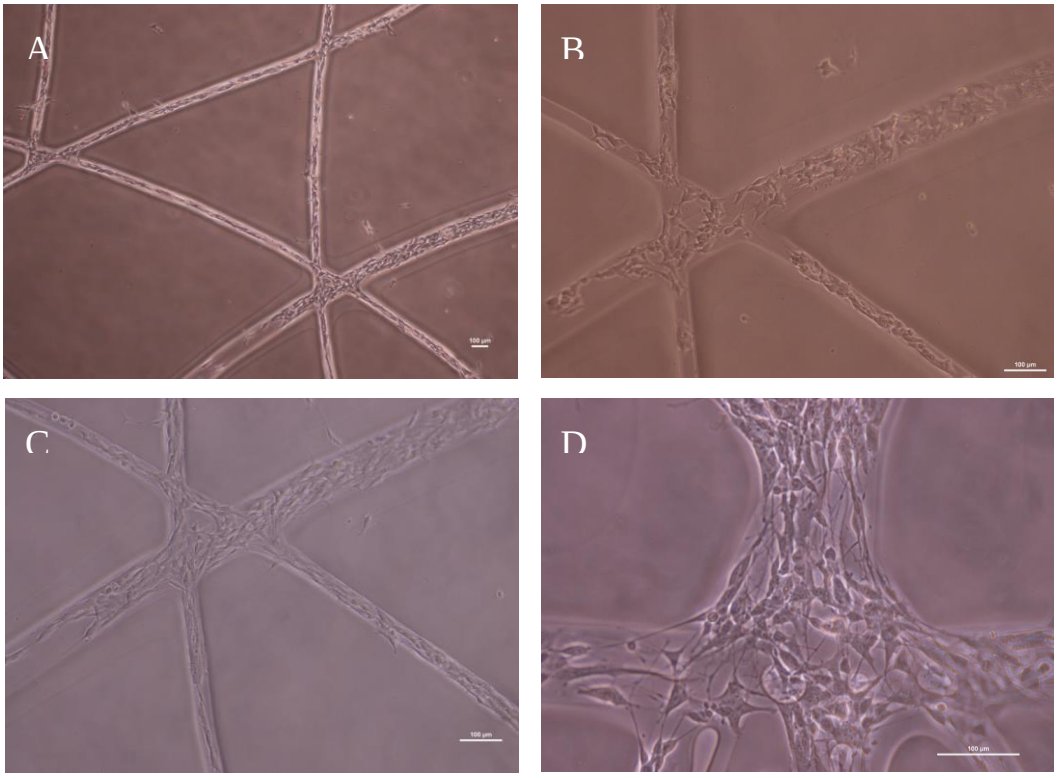

Figure 4.2: (a) Cells adhering specifically to 50 and 25 µm channels in an 'open architecture' and PEGDA resisting adhesion on day 2 (b) cells aligning in the channels before differentiation and starting to elongate (c) Adding RA induced neurites and showed further extension along the channels (d) High density of neurites visible at the intersection of channels.

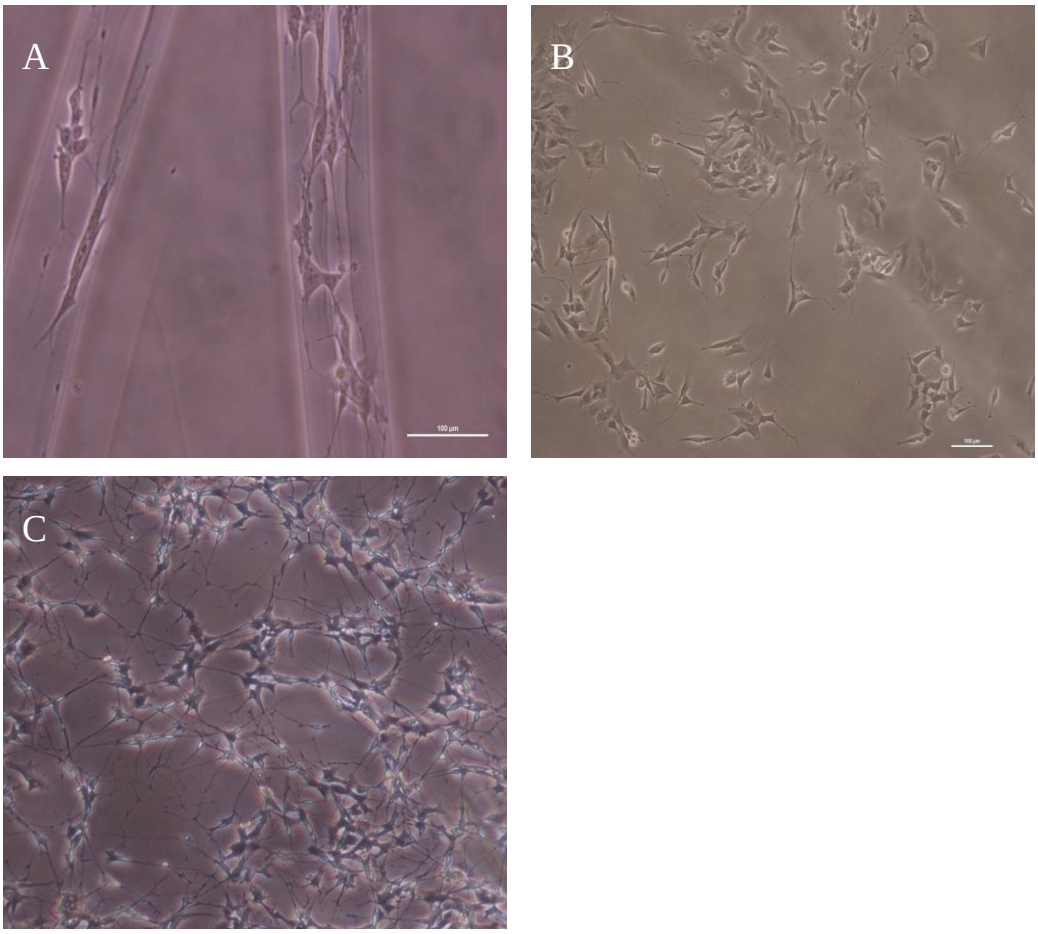

Figure 4.3: Images taken on day 5 with cells clearly developing neurites and appearing narrower in width in (a) the patterned channels and randomly oriented in the (b) TCP control and (c) Glass control.

The effect of architecture on changes in morphology compared to the unpatterned controls were quantified and statistically compared. This also gives an indication of the extent of neurite outgrowth in each case. **Figure 4.4** shows that the mean neurite length was significantly less on the patterned glass substrate than both controls (P^{*}<0.001). This is surprising since studies have consistently displayed substantial increases in neurite lengths with lanes and channels compared to open space [18, 19, 71]. It also does not quite match the observation indicated previously. For a more reliable result, a third trial is needed to form a triplicate and maybe a lower seeding

density to accurately make measurements inside the channels without any crowding. Adding the other soluble factors mentioned before and maybe providing more time for differentiation could yield the expected result. Total cell length also showed similar contradicting measurements since the mean was significantly less than both controls (P^{**}<0.001). The cell width was however as expected from the observed elongation of cell body inside the channels and exhibited significantly smaller widths compared to both controls ($P^{\#}$*<0.001).* It should also be noted that neurites occupied more than 65% of the total cell length in all three cases, which is a clear indication of differentiation. Measurements taken on open space for both controls had a much higher standard deviation particularly for neurite lengths which again confirms the randomness involved compared to the more organized and systematic structure provided by the features.

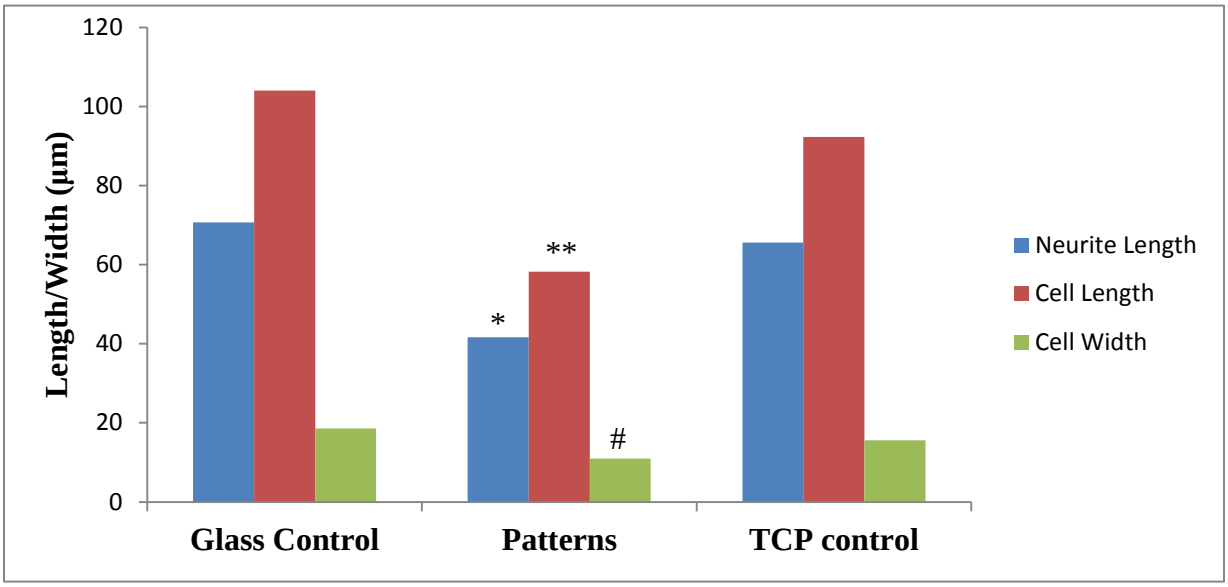

Figure 4.4: Neurite outgrowth was stimulated by RA and extent of differentiation is quantified through measurements of neurite length, cell length and cell width on the patterns, glass control and TCP control. Cell width is shown to be significantly lower in the patterns than both controls ($P^{\#}$<0.001) while neurite length and cell length were found to be significantly higher on the controls compared the patterned network (P^{*}<0.001 and P^{**}<0.001 respectively).

The stability of the PEGDA patterned glass sample was a significant issue when it came to cell staining. During cell culture the hydrogel was relatively stable in its attachment to the glass sample as long as it is stationary, but did show beginning of delamination at the corners after media changes. It was first assumed that the TPM treatment accounted for such detachment but samples were stable for weeks at room temperature and only exhibited such behavior at 37°C. It did not cope well with a dynamic environment involving changes in humidity and temperature even though increasing the composition of PEGDA from 40 wt% to 60 wt% was expected to show improved crosslinking and lower sensitivity to temperature due to having less water. The results presented thus far, point towards the need for functionality testing through immunochemistry and examining expression of neuron specific markers with each case to establish the extent of differentiation and resemblance to mature neurons.

4.3. Optimization of neural cell culture on 'open network' micropatterns

4.3.1 Human neural progenitors

Human neural progenitors (hNPs) were the first choice of cell to be differentiated on the micropatterned architectures. These cells act as an intermediate stage towards differentiation into motor neurons, sensory neurons or interneurons. The objective was to use topography to induce neural differentiation and increase its rate and yield. However, there were difficulties growing the cells on traditional tissue culture plates, particularly regarding their adhesion and proliferation. Initially the cells showed no signs of prolonged adhesion as they maintained a circular shape and failed to branch out, ultimately floating in the media as shown in **Figure 4.5(a).** In order to tackle this issue, approaches such as trying lower passage number lines,

increasing the laminin and poly-ornithine coating times and even plating all 1 million thawed cells on one dish. At best cells showed signs of proliferation on day 1 as seen in **Figure 4.5(b)** but would not grow confluent and eventually detach again.

Following these experiments, the conclusion was that there may have been an issue with the cell line. The neuroblastoma cell line SH-SY5Y were then selected for investigation. While these cells do not exhibit neuronal morphology and lack expression of neuron-specific markers, studies have shown that under certain conditions they are capable of generating high neuronal resemblance. Depending on the treatment the SH-SY5Y cells differentiate accordingly and certain stimuli like retinoic acid incorporated with physical confinement have already been proven to affect the morphology and neurite outgrowth. Another advantage is that these cells were grown with relative ease since they do not require coating on TCPs and proliferate quickly (**Figure 4.5**).

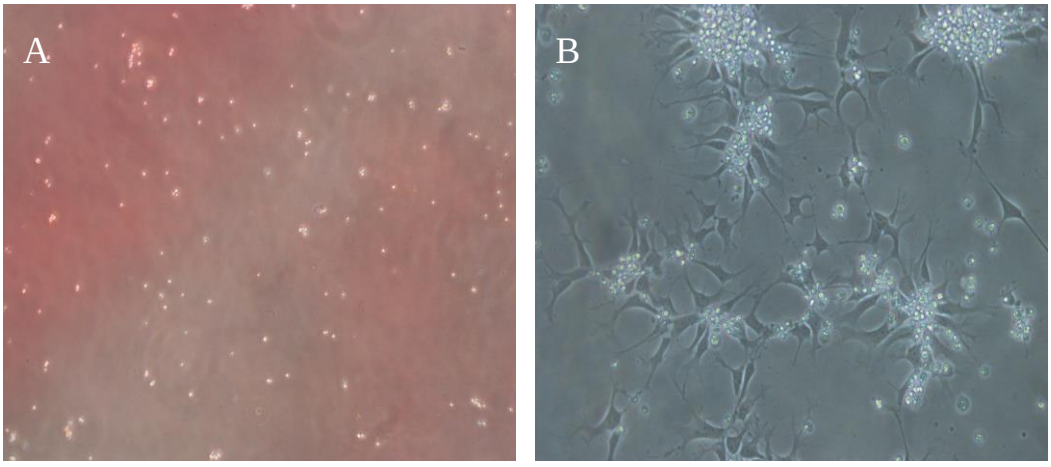

Figure 4.5: (a) Neural progenitors showing no signs of adhesion or proliferation but (b) started attaching and spreading with increased laminin and poly-ornithine coating times only to detach again on day 2.

4.3.1 Patterning on tissue-culture plate as a control.

To test the effect of the patterned architectures, irrespective of the substrate, on the differentiation of neuroblastoma cells and expression of neurons, it was attempted to repeat the features on tissue culture plate. Since contact lithography could not be used in this case, the PEGDA hydrogel needed to be very thin to ensure the features will reach the TCP surface. Spin coating was used to achieve such thickness uniformly, which also aids in the stability of the hydrogel as the hydrogel is not covalently attached to the TCP. Initial trials were not successful due to the hydrophobicity of the surface which hindered the flow of the added solution. Plates were then plasma treated for hydrophilicity which would allow the added solution to spread and still be convenient for cell culture. Single step spin coating was tried and showed clear improvement over the non-plasma treated surfaces. The added amount ranged from 200 to 300 μL and managed to almost coat the entire surface at a low speed of 200 rpm for 60 seconds. The layer however appeared to be irregular, which implied a second step might be needed to flatten it at a higher speed. Second steps ranging from 1000 to 2000 rpm were applied but ended up re-scattering the layer with the edges also beading up. Therefore, lower second step speeds were attempted next in order to achieve a thin uniform hydrogel upon exposure. Successful spin coating of 40% PEGDA solution was achieved on 60 mm tissue culture plates. The dish was plasma treated for 20 minutes prior to spin coating in order to make the surface temporarily hydrophilic. This allowed the solution to spread easily across the surface, forming a thin layer, and return to its hydrophobicity minutes after patterning, which is suitable for cell culture. 250-300 μL of the solution were added and spin coated at 150 rpm for 60 seconds in a one step process. Initially upon exposing the dish at a distance of 2 inches between the light source

substrate, only a portion of the layer got crosslinked regardless of the intensity and time (5% and 5-10 seconds). This indicated the distance needs to be increased to cover higher surface area but also an increase in exposure time to ensure polymerization. At a distance of 3 inches (covering the whole surface) and 5% intensity for 15 seconds, the entire surface was polymerized but with no sign of the features upon developing. Even though the distance permitted enough surface coverage by UV, it also meant higher light scattering, especially with the high distance already present between the photomask and substrate. Therefore, it was decided to focus on the glass patterned samples. However, it is noted that such a comparison would still be beneficial to illustrate the importance of the architecture with different substrates.

4.3.2 Culturing SH-SY5Y cells on micropatterned glass

Prior to achieving the specific adhesion shown in **Figure 4.2,** cells were first passaged on a glass sample patterned with 40 wt% PEGDA. Initially, fibronectin (10 µg/ml) was used included to coat the channels. Unexpectedly, despite the success of this composition to resist adhesion with fibroblasts, neuroblastoma cells adhered at high density to the hydrogel as seen in **Figure 4.6(a)**. Glass samples were patterned such that the 40% PEGDA hydrogel occupied half the substrate while the other half was exposed glass. Laminin was also examined as an alternative to fibronectin since it is known for inducing neurite outgrowth *in vitro* and is present in the ECM [70]. Therefore, the setup composed of a glass sample and control that have not been coated, primarily to check if the hydrogel is the issue, and two coated with laminin at a concentration of 6 µg/ml. **Figure 4.7(a)** shows that the laminin enabled the SH-SY5Y cells to attach to glass while the hydrogel was successful in resisting adhesion and was not affected by the coating. The

cells also surprisingly adhered to the uncoated glass sample at a higher density than with laminin as seen in **Figure 4.7(b)**. This was again confirmed on the uncoated glass control in **Figure 4.7(d)** which also had a high amount of cells adhered and proliferating compared to the laminin coated control in **Figure 4.7(c)**. The cells were therefore patterned once again on the 'open network' structure without coating the samples and it did reduce the amount of cells adhering to the hydrogel as seen in **Figure 4.6(b).** While there were cells present inside the channels, the majority concentrated outside in the open space and continued to grow on the hydrogel. They even differentiated with the introduction of RA. This could also be attributed the large area that was available for adhesion on the tests compared to the network patterned substrates. To further remedy the situation, the PEGDA composition was finally increased to 60 wt% which brought about the results presented previously in **Figure 4.2.**

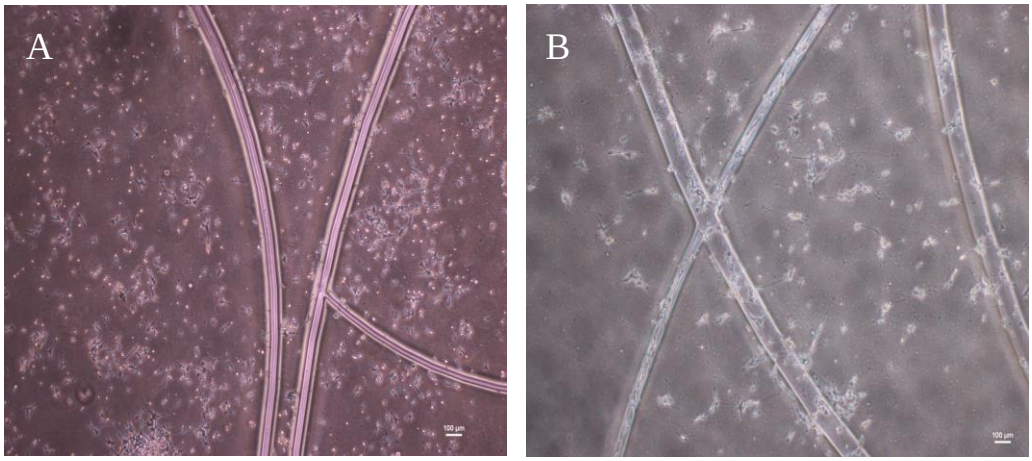

Figure 4.6: (a) Cells adhered at a high density to the 40 wt% PEGDA hydrogel following coating the sample with fibronectin at 10 µg/ml. (b) An uncoated sample showed reduction in adhesion to the hydrogel but was still higher than the channels.

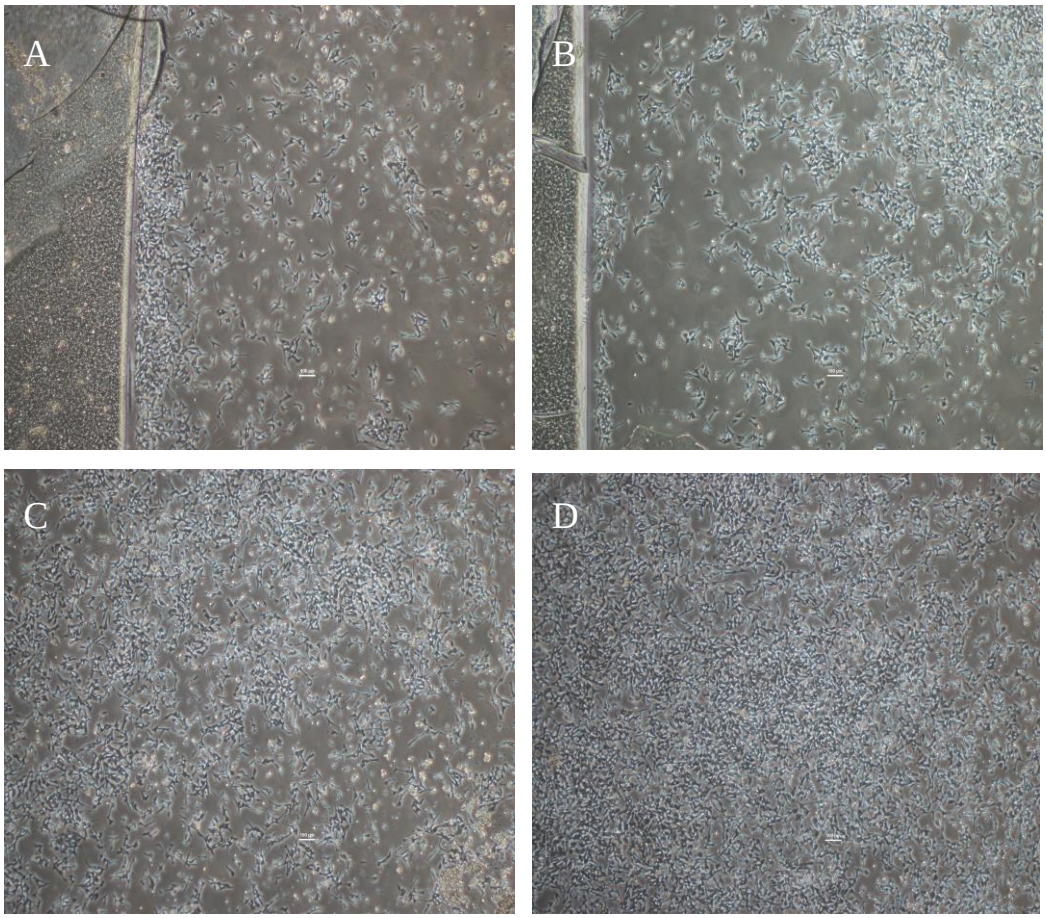

Figure 4.7: Test experiment conducted with SH-SY5Y cells on (a) Laminin coated glass sample with 40 wt% PEGDA hydrogel occupying half the substrate (b) Uncoated glass sample patterned the same way (c) Laminin coated glass control (d) uncoated glass control.

4.4. Conclusion

Neuroblastoma cells were successfully patterned in complex networks that potentially mimic natural neuronal architectures beyond the simpler features demonstrated in previous studies. Increasing the PEGDA concentration to 60% helped achieve more specific adhesion to the channels over an area of 0.8 inch^2. Upon differentiation, the topography resulted in reducing the width of the cells with neurites occupying most of the cell area and elongation clearly visible along the channels. The neurite lengths and percentage occupied of the cell were fairly similar to results on open space controls on glass and TCPs. Intersections in the open networks exhibited a clear high density of neurites connecting the cells which adapted to the changes in directions. While the glass samples demonstrated consistent patterning and the hydrogel was stable enough to last for 7 days cultures, they tended to fall apart during the staining and fixation steps which followed. PDMS on the other hand, while more difficult to pattern regularly with complex features, was able to withstand environmental changes and last for longer periods of time. Therefore, in order to achieve the next stage for a complete study and to test functionality of the differentiated cells in terms of biological markers, further work is needed on either improving the stability of the PEGDA hydrogels on glass or patterning more consistently on PDMS.

Chapter 5: Conclusions and future direction

5.1. Conclusions

Integrating microfabrication and cell culture continues to evolve with increasing applications in the medical and biological directions. In order to reach its full potential and reach highly efficient, directed cellular response, more uniform cell patterning over large areas is a requirement. In this study we were able to introduce a method consisting of a combination of various techniques for micropatterning cells on PDMS particularly due to its advantages as a biocompatible substrate. Poly (ethylene glycol) diacrylate (PEG-DA) was used to resist protein and cell adhesion by forming a physical and chemical barrier around the photografted patterns. Large areas up to 1 inch^2 were obtained which is an important criterion for future tissue engineering applications. The patterned PDMS substrates exhibited high stability and offered precise protein adhesion to grafted channels. Controlled cell adhesion and proliferation was also demonstrated on 10:1, 20:1 and 5:1 PDMS to examine the effect of stiffness and fibroblasts were found to grow optimally on 10:1 PDMS by exhibiting the highest cell density. This supported claims that cells respond to the mechanical properties of substrates in general and the stiffness of PDMS in particular. It also showed the repeatability of the suggested mechanism on different ratios of PDMS with 10:1 being the favored option in terms of high patterning area, stiffness and crosslinking density. However, consistency was not true with more complex spatial designs beyond traditional patterns and grids since micropatterning and exposure parameters had to be fluctuated throughout trials. Since this factor is also vital for tissue engineering and regenerative

medicine applications, glass was used next as an alternative since it showed more regularity and ability to pattern various features down to 10 μm with a straight forward protocol.

This allowed investigation of features that mimic biological networks through "open architectures" on neuronal cell lines by spreading them out in an interconnected network similar to the *in vivo* environment. The neuroblastoma cell line SH-SY5Y was the focus of this study in terms of attempting to use the proposed geometry to bring the differentiated cell line closer to displaying characteristics of mature neurons. Cells were cultured on the networks and precisely adhered to the glass channels of sizes 50 and 25 μm. Upon differentiation using retinoic acid the cells exhibited visible neurite outgrowth with the neurites occupying most of the cell length. Cell widths were found to be significantly lower in the channels as expected due to the tangential elongation. However, neurite and total cell lengths were surprisingly higher on glass and TCP controls and did not quite represent the visible and proven effect of topography that has been previously observed on various studies for even simpler structures. However, the intersections available in this network, as opposed to parallel lanes, showed a high density of neurites connecting the cells from various directions. This can be a strategy to promote optimal growth towards neural regeneration.

5.2. Future Directions

Future work can involve improving the stability of the PEGDA hydrogel on glass so it can sustain staining and even longer periods of differentiation. A different approach for inducing

neurite outgrowth may be attempted which involves RA pretreatment for one week followed in the inclusion of brain derived neurotrophic factor, neuregulin B1, nerve growth factor and vitamin D3 to further stimulate neurite branching and increase in length. Further measurements can be added to the reported ones and ensuring the consistency of these results while also examining if they will differ given the new differentiation approach suggested.

Immunochemistry to test expression of neurospecific markers such as the nuclear marker NeuN which RA treated cells are usually negative for and would be interesting to see if the network pattern would increase its intensity. The architectures designed on the photomask with varying surface areas can also be a next step to compare how the cells would respond and if there is a systematic reaction to the density of adhesion sites available. Channel sizes lower than 25 μm ought to be included in the cell culture too since it has been previously suggested that such low width lanes stimulated neurite outgrowth beyond adding RA alone. TCP patterning if possible could also validate the influence of 'open networks" irrespective of the substrate used. If PDMS can also be micropatterned consistently with these complex features through a fixed protocol it would solve the stability issues faced with glass and provide the biocompatible, gas permeable, flexible substrate originally required. Finally, optimizing the differentiation of neuroblastoma cells on these architectures should bring them a step closer to providing insight on the mechanisms behind various neurological disorders through a more accurate, biomimetic model. Micropatterning neural progenitors in such an organized, interconnected manner would even be a step further in tissue engineering and efforts to regenerate damaged neurons.

References

1. Liu, W.W., Z.L. Chen, and X.Y. Jiang, *Methods for Cell Micropatterning on Two-Dimensional Surfaces and Their Applications in Biology.* Chinese Journal of Analytical Chemistry, 2009. **37**(7): p. 943-949.
2. Walker, G.M., H.C. Zeringue, and D.J. Beebe, *Microenvironment design considerations for cellular scale studies.* Lab on a Chip, 2004. **4**(2): p. 91-97.
3. Jiang, X.a.W., G.M., *Engineering Microtools in Polymers to Study Cell Biology.* Engineering in Life Sciences, 2003. **3**(12): p. 475-480.
4. Folch, A. and M. Toner, *Microengineering of cellular interactions.* Annual review of biomedical engineering, 2000. **2**(1): p. 227-256.
5. Hosseinkhani, M., et al., *Engineering of the embryonic and adult stem cell niches.* Iran Red Crescent Med J, 2013. **15**(2): p. 83-92.
6. Yap, F.L. and Y. Zhang, *Protein and cell micropatterning and its integration with micro/nanoparticles assembly.* Biosensors & Bioelectronics, 2007. **22**(6): p. 775-788.
7. Revzin, A., R.G. Tompkins, and M. Toner, *Surface engineering with poly(ethylene glycol) photolithography to create high-density cell arrays on glass.* Langmuir, 2003. **19**(23): p. 9855-9862.
8. Sugaya, S., et al., *Micropatterning of Hydrogels on Locally Hydrophilized Regions on PDMS by Stepwise Solution Dipping and in Situ Gelation.* Langmuir, 2012. **28**(39): p. 14073-14080.
9. Choi, J.H., et al., *Micropatterning of neural stem cells and Purkinje neurons using a polydimethylsiloxane (PDMS) stencil.* Lab on a Chip, 2012. **12**(23): p. 5045-5050.
10. Goudar, V.S., S. Suran, and M.M. Varma, *Photoresist functionalisation method for high-density protein microarrays using photolithography.* Micro & Nano Letters, 2012. **7**(6): p. 549-553.
11. Ross, A.M. and J. Lahann, *Surface engineering the cellular microenvironment via patterning and gradients.* Journal of Polymer Science Part B: Polymer Physics, 2013. **51**(10): p. 775-794.
12. Teixeira, A.I., et al., *Epithelial contact guidance on well-defined micro- and nanostructured substrates.* Journal of Cell Science, 2003. **116**(10): p. 1881-1892.
13. Anderson, D.E.J. and M.T. Hinds, *Endothelial Cell Micropatterning: Methods, Effects, and Applications.* Annals of Biomedical Engineering, 2011. **39**(9): p. 2329-2345.
14. Chen, C.S., et al., *Micropatterned Surfaces for Control of Cell Shape, Position, and Function.* Biotechnology Progress, 1998. **14**(3): p. 356-363.
15. Kane, R.S., et al., *Patterning proteins and cells using soft lithography.* Biomaterials, 1999. **20**(23-24): p. 2363-2376.
16. Tsuda, Y., et al., *The use of patterned dual thermoresponsive surfaces for the collective recovery as co-cultured cell sheets.* Biomaterials, 2005. **26**(14): p. 1885-1893.
17. Bhatia, S., et al., *Effect of cell–cell interactions in preservation of cellular phenotype: cocultivation of hepatocytes and nonparenchymal cells.* The FASEB Journal, 1999. **13**(14): p. 1883-1900.

18. Chan, L.Y., et al., *Temporal application of topography to increase the rate of neural differentiation from human pluripotent stem cells.* Biomaterials, 2013. **34**(2): p. 382-92.
19. Mahairaki, V., et al., *Nanofiber matrices promote the neuronal differentiation of human embryonic stem cell-derived neural precursors in vitro.* Tissue Eng Part A, 2011. **17**(5-6): p. 855-63.
20. Metallo, C.M., et al., *Engineering the stem cell microenvironment.* Biotechnol Prog, 2007. **23**(1): p. 18-23.
21. Annabi, N., et al., *Highly Elastic Micropatterned Hydrogel for Engineering Functional Cardiac Tissue.* Advanced Functional Materials, 2013. **23**(39): p. 4950-4959.
22. Vasiev, I., et al., *Self-folding nano- and micropatterned hydrogel tissue engineering scaffolds by single step photolithographic process.* Microelectronic Engineering, 2013. **108**: p. 76-81.
23. Lee, H., et al., *Application of cellular micropatterns to miniaturized cell-based biosensor.* Biomedical Engineering Letters, 2013. **3**(3): p. 117-130.
24. Koh, W.-G. and M. Pishko, *Fabrication of cell-containing hydrogel microstructures inside microfluidic devices that can be used as cell-based biosensors.* Analytical and Bioanalytical Chemistry, 2006. **385**(8): p. 1389-1397.
25. Pancrazio, J., et al., *Development and application of cell-based biosensors.* Annals of biomedical engineering, 1999. **27**(6): p. 697-711.
26. Falconnet, D., et al., *Surface engineering approaches to micropattern surfaces for cell-based assays.* Biomaterials, 2006. **27**(16): p. 3044-3063.
27. Bhatnagar, P., et al., *Multiplexed protein patterns on a photosensitive hydrophilic polymer matrix.* Adv Mater, 2010. **22**(11): p. 1242-6.
28. Takahashi, H., et al., *Micropatterned Thermoresponsive Polymer Brush Surfaces for Fabricating Cell Sheets with Well-Controlled Orientational Structures.* Biomacromolecules, 2011. **12**(5): p. 1414-1418.
29. Hahn, M.S., et al., *Photolithographic patterning of polyethylene glycol hydrogels.* Biomaterials, 2006. **27**(12): p. 2519-2524.
30. Sugiura, S., et al., *Surface modification of polydimethylsiloxane with photo-grafted poly(ethylene glycol) for micropatterned protein adsorption and cell adhesion.* Colloids and Surfaces B: Biointerfaces, 2008. **63**(2): p. 301-305.
31. Wang, Y.L., et al., *Covalent micropatterning of poly(dimethylsiloxane) by photografting through a mask.* Analytical Chemistry, 2005. **77**(23): p. 7539-7546.
32. Wang, L., et al., *Chemical and physical modifications to poly(dimethylsiloxane) surfaces affect adhesion of Caco-2 cells.* Journal of Biomedical Materials Research Part A, 2009. **93A**(4): p. 1260-1271.
33. Chen, W., R.H.W. Lam, and J. Fu, *Photolithographic surface micromachining of polydimethylsiloxane (PDMS).* Lab on a Chip, 2012. **12**(2): p. 391-395.
34. Lee, J.N., et al., *Compatibility of Mammalian Cells on Surfaces of Poly(dimethylsiloxane).* Langmuir, 2004. **20**(26): p. 11684-11691.
35. DECKER, C., *Photoinitiated crosslinking polymerisation.* Progress in polymer science, 1996. **21**(4): p. 593-650.
36. Beduer, A., et al., *Engineering of adult human neural stem cells differentiation through surface micropatterning.* Biomaterials, 2011. **33**(2): p. 504-514.

37. de Silva, M., R. desai, and D. Odde, *Micro-Patterning of Animal Cells on PDMS Substrates in the Presence of Serum without Use of Adhesion Inhibitors.* Biomedical Microdevices, 2004. **6**(3): p. 219-222.
38. Whitesides, G.M., et al., *Soft lithography in biology and biochemistry.* Annual Review of Biomedical Engineering, 2001. **3**: p. 335-373.
39. Xu, Y., et al., *Microchip-based cellular biochemical systems for practical applications and fundamental research: from microfluidics to nanofluidics.* Analytical and Bioanalytical Chemistry, 2012. **402**(1): p. 99-107.
40. Sia, S.K. and G.M. Whitesides, *Microfluidic devices fabricated in poly(dimethylsiloxane) for biological studies.* Electrophoresis, 2003. **24**(21): p. 3563-3576.
41. Dalby, M.J., et al., *Changes in fibroblast morphology in response to nano-columns produced by colloidal lithography.* Biomaterials, 2004. **25**(23): p. 5415-5422.
42. Kang, K., et al., *Generation of Patterned Neuronal Networks on Cell-Repellant Poly(oligo(ethylene glycol) Methacrylate) Films.* Chemistry-an Asian Journal, 2010. **5**(8): p. 1804-1809.
43. Rogers, C.I., et al., *Single-Monomer Formulation of Polymerized Polyethylene Glycol Diacrylate as a Nonadsorptive Material for Microfluidics.* Analytical Chemistry, 2011. **83**(16): p. 6418-6425.
44. Harris, J.M. and S. Zalipsky, *Poly (ethylene glycol)*. 1997: American Chemical Society.
45. Koh, W.-G., et al., *Control of Mammalian Cell and Bacteria Adhesion on Substrates Micropatterned with Poly(ethylene glycol) Hydrogels.* Biomedical Microdevices, 2003. **5**(1): p. 11-19.
46. Schlapak, R., et al., *Glass Surfaces Grafted with High-Density Poly(ethylene glycol) as Substrates for DNA Oligonucleotide Microarrays.* Langmuir, 2005. **22**(1): p. 277-285.
47. Rhee, S.W., et al., *Patterned cell culture inside microfluidic devices.* Lab Chip, 2005. **5**(1): p. 102-7.
48. Patrito, N., et al., *Spatially controlled cell adhesion via micropatterned surface modification of poly(dimethylsiloxane).* Langmuir, 2007. **23**(2): p. 715-9.
49. Bodas, D. and C. Khan-Malek, *Formation of more stable hydrophilic surfaces of PDMS by plasma and chemical treatments.* Microelectron. Eng., 2006. **83**(4-9): p. 1277-1279.
50. Hutter, J.L. and J. Bechhoefer, *Calibration of atomic-force microscope tips.* Review of Scientific Instruments, 1993. **64**(7): p. 1868-1873.
51. Oliver, W.C. and G.M. Pharr, *Measurement of hardness and elastic modulus by instrumented indentation: Advances in understanding and refinements to methodology.* Journal of Materials Research, 2004. **19**(1): p. 3-20.
52. Almutairi, Z., C.L. Ren, and L. Simon, *Evaluation of polydimethylsiloxane (PDMS) surface modification approaches for microfluidic applications.* Colloids and Surfaces A: Physicochemical and Engineering Aspects, 2012. **415**(0): p. 406-412.
53. Eroshenko, N., et al., *Effect of substrate stiffness on early human embryonic stem cell differentiation.* J Biol Eng, 2013. **7**(1): p. 7.
54. Brown, X.Q., K. Ookawa, and J.Y. Wong, *Evaluation of polydimethylsiloxane scaffolds with physiologically-relevant elastic moduli: interplay of substrate mechanics and surface chemistry effects on vascular smooth muscle cell response.* Biomaterials, 2005. **26**(16): p. 3123-3129.

55. Carrillo, F., et al., *Nanoindentation of polydimethylsiloxane elastomers: Effect of crosslinking, work of adhesion, and fluid environment on elastic modulus.* Journal of Materials Research, 2005. **20**(10): p. 2820-2830.
56. Mata, A., A.J. Fleischman, and S. Roy, *Characterization of polydimethylsiloxane (PDMS) properties for biomedical micro/nanosystems.* Biomed Microdevices, 2005. **7**(4): p. 281-93.
57. Schneider, M.H., Y. Tran, and P. Tabeling, *Benzophenone absorption and diffusion in poly(dimethylsiloxane) and its role in graft photo-polymerization for surface modification.* Langmuir, 2011. **27**(3): p. 1232-40.
58. Lee, J.N., C. Park, and G.M. Whitesides, *Solvent Compatibility of Poly(dimethylsiloxane)-Based Microfluidic Devices.* Analytical Chemistry, 2003. **75**(23): p. 6544-6554.
59. Park, J.Y., et al., *Surface chemistry modification of PDMS elastomers with boiling water improves cellular adhesion.* Sensors and Actuators B: Chemical, 2012. **173**(0): p. 765-771.
60. Wu, M.-H., *Simple poly(dimethylsiloxane) surface modification to control cell adhesion.* Surface and Interface Analysis, 2009. **41**(1): p. 11-16.
61. Leipzig, N.D. and M.S. Shoichet, *The effect of substrate stiffness on adult neural stem cell behavior.* Biomaterials, 2009. **30**(36): p. 6867-6878.
62. Seo, J.-H., K. Sakai, and N. Yui, *Adsorption state of fibronectin on poly(dimethylsiloxane) surfaces with varied stiffness can dominate adhesion density of fibroblasts.* Acta Biomaterialia, 2013. **9**(3): p. 5493-5501.
63. Abraham, S., et al., *Characterization of human fibroblast-derived extracellular matrix components for human pluripotent stem cell propagation.* Acta Biomaterialia, 2010. **6**(12): p. 4622-4633.
64. Anadon, A., *Toxicological evaluation of benzophenone.* The EFSA Journal, 2009: p. 1-30.
65. Lo, C.M., et al., *Cell movement is guided by the rigidity of the substrate.* Biophys J, 2000. **79**(1): p. 144-52.
66. Zhao, C., et al., *Nanomaterial scaffolds for stem cell proliferation and differentiation in tissue engineering.* Biotechnol Adv, 2013. **31**(5): p. 654-68.
67. Higgins, S., et al., *Inducing neurite outgrowth by mechanical cell stretch.* Biores Open Access, 2013. **2**(3): p. 212-6.
68. Agholme, L., et al., *An in vitro model for neuroscience: differentiation of SH-SY5Y cells into cells with morphological and biochemical characteristics of mature neurons.* J Alzheimers Dis, 2010. **20**(4): p. 1069-82.
69. Delivopoulos, E., et al., *Guided growth of neurons and glia using microfabricated patterns of parylene-C on a SiO2 background.* Biomaterials, 2009. **30**(11): p. 2048-58.
70. Dwane, S., E. Durack, and P.A. Kiely, *Optimising parameters for the differentiation of SH-SY5Y cells to study cell adhesion and cell migration.* BMC Res Notes, 2013. **6**: p. 366.
71. Poudel, I., et al., *Micropatterning-retinoic acid co-control of neuronal cell morphology and neurite outgrowth.* Acta Biomater, 2013. **9**(1): p. 4592-8.

72. Xie, H.R., L.S. Hu, and G.Y. Li, *SH-SY5Y human neuroblastoma cell line: in vitro cell model of dopaminergic neurons in Parkinson's disease.* Chin Med J (Engl), 2010. **123**(8): p. 1086-92.